Reviewer 1

The manuscript of Rasbury et al describes a toolkit for U-Pb geochronology and specif-ically presents characterization of a couple of used or potentially applicable reference materials. The methods are up to date, although some commonly used characteriza-tion methods for natural samples are missing. The discussion about U speciation is interesting but requires some more connection to published findings of high U incor-poration of U into calcite. I think this manuscript can be published after some minor revisions. Specifically important is the measurements of U(IV) in the calcites, but some more discussion on how the U speciation affect geochronology considerations and re-sults could be suitable. A minor setback is that discussions of processes of U speciation and incorporation and suitability of and heterogeneity of different reference materials are mixed and make the paper a bit un-distinct in its focus.

To our knowledge, the manuscript has referred to all of the published work on the oxidation state of U in carbonates. There is really no evidence that it matters for dating if the U is reduced or oxidized. Rather, the question is how is uranium available to be incorporated. For the three examples we present, we suggested how the uranium was available. To address this concern though, we state up front now that there is no evidence that the oxidation state of uranium matters to the reliability for U-Pb dating.

We added: 'Understanding U incorporation in carbonates is important for a holistic approach to U-Pb dating, but there is no evidence that the oxidation state of U in carbonates has any control on the reliability of the dating. However, it could indicate something about when during diagenesis the U was incorporated, and therefore affect the interpretation of the U/Pb date'

Specific c omments: T itle: I t w ould b e g ood i f t he t itle s pecifies th at it is ca lcite and dolomite that is in focus of this manuscript as there are many other minerals under the "carbonate" umbrella. Title and throughout the MS: consider changing "standards" to "reference materials".

While it is true that we only discussed calcite and dolomite in this contribution, we would argue that the tools are also relevant to other carbonates, and would rather the title be broader so that researchers that are analyzing any carbonate, particularly oneS that they would like to date, would find our paper.

We agree that the use of reference materials is more accurate than standards and this has been globally replaced.

Abstract: It would be helpful if it was stated whether the "split stream" analysis of 87Sr/86Sr together with U/Pb, is done with LA-ICP in the same spot, in nearby spots, or if the 87Sr/86Sr is done on dissolved samples and U/Pb with spot analysis. And, if it is the latter, the later discussion should discuss how the difference in scale of larger dissolved aliquotes match spots, when taking heterogeneity of the material into account.

We have not done split stream analyses. The beauty of split stream though, is that it can be done on the same spots. Our 87Sr/86Sr results are from Thermal Ionization Mass Spectroscopy and the range of values obtained is included to make these possible reference materials available for split stream for those labs that are set up for it.

We added 'While not part of the current contribution, this combination could streamline split stream analyses of 87Sr/86Sr and U/Pb geochronology'. to clarify this to the reader.

Line 20-21: "Mixing of fluids can be particularly corrosive or can be responsible for mineral precipitation." please give more details.

Lines 21 and onwards: "Introduction of C2fluids with different chemistries through uplift or burial can destroy the original carbonate prior to precipitation of a new carbonate

These two comments are coupled and are addressed together here. We added to this statement to clarify, and we added important references for papers that are foundational to this statement.

Mixing of fluids can be particularly corrosive such as seen where seawater and fresh water mix in a carbonate platform, or can be responsible for mineral precipitation depending on the saturation state of the combined fluids \citep{runnells_diagenesis_1969, wigley_mixing_1976}.

Lines 55-58: "Laser ablation mapping (Woodhead et al., 2010, 2007; Piccione et al., 2019; Drost et al., 2018; Roberts et al., 2020), synchrotron XRF mapping (Cole et al., 2004; Piccione et al., 2019; Frisia et al., 2008; Vanghi et al., 2019), PIXE (Ortega et al., 2005, 2003) and μXRF (de Winter et al., 2017) are all ways to take the physical observations of different phases to a new level with in situ chemistry, that maps U in particular, along with other elements that provide details of the fluid chemistry." It would also be good to add the FE-EMPA for spatial characterization of presence of U nano-particles in calcite (see Suzuki et al., 2016 SciRep).

Thanks. We added this reference in the context suggested here.

Because the uranium in this contribution is not in the calcite lattice, but rather U mineral nano-inclusions we added this as well: 'In some cases, uranium minerals are encapsulated in calcite which can protect them from alteration \citet{suzuki_formation_2016,ludwig_uranium-daughter_1978}.'

Lines 61-65: "Given that the major element composition of seawater has changed appreciably through time (Hardie, 1996; Horita et al., 2002), that meteoric fluid com-positions are controlled by water rock interaction (Chung and Swart, 1990) and that deep brines have evolved since deposition in basins (Musgrove and Banner, 1993), we can imagine that there is no such thing as a typical fluid. A holistic approach to dating carbonates should involve an effort to see back to the fluid or fluids that have been responsible for its formation and how they might have changed through the diagenetic history."

At some point in the introduction or in the other text, that surch for growth zonations using SEM, CL, and SIMS C- and O-isotope analyses prior to dating. see Milodowski et al APGEO https://www.sciencedirect.com/science/article/pii/S0883292718301938, and Drake et al NatComm 2019 https://www.nature.com/articles/s41467-019-12728-y. What also could be included in a toolbox for complex samples are fluid inclusion studies that can tell about mixing at particular events and about different fluid flow events

by giving T and salinity estimates. Another tool is in situ Sr isotope values of different growth zones of calcite crystals. see Drake et al., 2019 for the latter.

We agree that all of these tools are important for a full characterization of carbonates and clumped isotopes are useful as well. Many techniques are applicable to characterize the cement stratigraphy of samples. We rephrased our introductory paragraph on techniques to read as follows:

"Often, combining microanalytical tools that characterize carbonates at the micron to centimeter scale of growth zones is required to understand the origin and timing of various textures in complex samples. Chemical imaging techniques, carbonate staining, and polarized light, fluorescence, electron, and cathodoluminescence microscopy provide spatial context for quantitative microscale analyses of fluid inclusion, ion microprobe, electron microprobe, and laser ablation measurements. Integrated data from such a toolkit enables collection of LA-U/Pb isochrons that reliably date a single paragenetic event and permits geologically meaningful interpretation of U/Pb ages."

Line 129-130: "The cements have mostly been altered to calcite, though Chafetz et al.(2008) found original aragonite in similar cements. Calcite with the greatest alteration is light brown..." This is a bit unclear, is the light brown calcite the most altered of the calcites, or is it replacing aragonite to a larger degree than other calcite types does?

It is almost all calcite as stated : The Walnut Canyon sample has incredible preservation of the original fibrous aragonite texture even though it is almost entirely converted to calcite. We added:

"While optical orientation is preserved and fluid inclusions and aragonite relict mineral inclusions delineate the original acicular growth habit, the carbonate is almost entirely replaced by cloudy brown calcite (Mazzullo 1980)."

Mazzullo, S. J. "Calcite Pseudospar Replacive of Marine Acicular Aragonite, and Implications for Aragonite Cement Diagenesis." *Journal of Sedimentary Research* 50, no. 2 (June 1, 1980): 409–22. https://doi.org/10.1306/212f7a18-2b24-11d7-8648000102c1865d.

Line 131: "WC-1", mention "Walnut Canyon" at first mention of this material.

Done

Line 135: Fig 3: quality of figure is not publishable. Maybe this has to do with compres-sion for pdf conversion. The veins are difficult to see.

Rescanned and grouped with former Fig. 4

Lines 139-140: "Cathodoluminescence (CL) has been a go-to test for diagenesis, and when an activator such as Mn is present, this often gives phenomenal images that illu-minate alteration." and is also very good for veins and single crystals in open fractures, to track different events of precipitation and/or reacitvation and fluid flow fluctuations.

Agreed, and added. Thank you.

Line 144: Fig. 4, 5, 6: These are nice figures, some suggestions; 1. however, what is the difference between Fig 4a, and 5a Since fig 4b and "5-Sr" are the same, maybe 4 can be deleted and 4a inserted (if it is not the same as 5-"photo" but in B&W, the caption does not say.) 2. What is roughly the range of Sr concentrations in these figures (4-5)? It would be very interesting to know as there is also clear drop in Ca in the Sr-rich parts, so I assume Sr concentrations are quite high.

Figure 4a (top) is a CL image of the slab shown in Figure 3. The only overlap in images is that 5Sr is indeed the same as the one we paired with the CL in figure 4. We think it is nice to have it in both places because it is easier to see how it relates to other elements when they are side by side as in Fig 5, but a major point is that the Sr map does a better job of showing alteration than the CL so having them paired together in 4 and blown up to make it easier to convey that seems justified. We are suggesting that as a reference material, we think that maps of each slab and only using areas that are the least altered (which is still more than half of the slab) would result in better reproducibility of measurements of this reference material.

Line 160: Fig 7: This figure is nice, but would to readers (such as me) who reads from left to write, be more logic if starting at left (old) towards right (young). How were the aliquots for Sr prepared, micro-drill, or are they in situ analyses using LA-MC-ICP-MS?details can be given here.

It is certainly reasonable to reflect this graph so that older is on the left- so we changed it as suggested. We added 'The aliquots were microsampled, dissolved and purified using Sr spec resin, and run by Thermal Ionization Mass Spectrometry' to the figure caption. We also changed the scales to zoom in a bit and added a line that is the average of 1, 3, 4, 5 and for the 2SD of that average. While 2 isn't included in the average it plots on the lower line. We left out the tiny slabs of the rock because it isn't possible to make them easy to see and they are described.

Line 160: "...with an average of 0.706930(69)", what is "(69)"? a reference with wrong formatting?

We changed this throughout the text to (0.000069). It is a somewhat normal convention to leave the zeros off but since it was confusing to the reviewer it makes sense to be as clear as possible.

Line 165: "...in seawater through the growth of the cements." Here, fluid inclusions may be useful to give more information on the history of fluids and alteration.

We agree with this and this reviewer is right on target with these comments. However, we start the sentence that without more work it isn't possible to know, and it seems off target to put too much more emphases on this point.

Line 169: TES: define, both in terms of settings and acronym

We do define this in the early section on synchrotron measurements starting on line 94. However, we had not done a good job of talking about the settings so we added a section about the energy range this represents. It now reads:

'These brighter sources offer micron sized resolution for low ppm levels of the elements of interest. Emerging tender energy spectroscopy (TES), using the energy range between soft and hard Xray techniques allows mapping of elements such as Mg and S that are important in carbonates \citep{northrup_tes_2019}.'

Line 173: fig 8, add to caption which sample it is

Done- it is Walnut Canyon and we state that it is the same slab shown in Fig. 3-6.

Line 179-180: "Through neomorphism to calcite, U was left behind because active functional groups such as carboxyl have a high affinity for uranyl." So was uranyl com- plexed to carboxyl in the primary fluid and incorporated into aragonite as carboxyl-complexes. Or did this complexation occur after recrystallization? if the former, could the aragonites have had exceptional U/Sr already at the aragonite stage?

This is a good question. Aragonite doesn't exclude U, but we don't know the U concentration or U/Ca ratio of Permian seawater so we can't know this. There is certainly abundant organic matter and whether the active functional groups represent the degradation products of the original organisms that produced them, or if these were organic molecules that were structurally incorporated is not possible to know. As written, we imply that the U was incorporated in the aragonite and then retained because of this affinity for the organic acid functional groups. We didn't change anything, but if we missed the point of the question we will be happy to revisit it.

Line 189-191; this sentence is not comprehensive, something is missing. and full reference should not be within ().

We fixed the parenthesis and we reworded the sentences relevant to this comment to make it clear we are characterizing a new sample that is large enough to share with the community.

'The sample that we are using to illustrate these tools for characterization is large enough to be suitable for distribution as a secondary reference material for LA carbonate dating (Fig. \ref{fig:BarstowTufa}). Most of the samples used in the \citet{cole_using_2005} study were small slabs from Vicki Pedone (Cal State Northridge) and are too limited in quantity to distribute to the community. Here, we are characterizing a new sample that is large enough to distribute widely.'

Lines 192-193: "Isotope dilution on this sample is under way and will be completed when Covid quarantine is lifted." Such a phrase makes me question if this something that will be included in this MS at revision, otherwise this level of details is probably not adding anything.

AGREE WE WILL EITHER FINISH THIS DATA OR DELETE THE STATEMENT AT SUBMISSION OF THE MANUSCRIPT.

Lines 198-199: "there are mm to cm scale layers of higher and lower U concentrations (Cole et al., 2004)." what are these concentrations: "higher" and "lower"?

We added approximate concentrations in parentheses. 'citet{becker_cyclic_2001} showed that layers in the Barstow tufa deposits have a pattern of low (~10ppm) to high (several hundred ppm) U concentrations across laminae revealed by fission track mapping.'

Line 207: "The 87Sr/86Sr isotope ratios are similar throughout the sample..." this is a bit unspecific. maybe say "show relatively small variability" because there is indeed some variability

This is true and we have changed the wording to be more accurate.

'The 87Sr/86Sr isotope ratios of 3 aliquots ranged from 0.719877 to 0.721038 (Table \ref{tab:BT_Sr})'.

Line 209; "...making it a good Sr isotope standard..." I am not certain that the three analyses presented here are enough to state it is a suitable standard for Sr isotope analysis. It is stated that zones with high Sr would narrow the range (also for Sr isotope variability?), I cannot see how this is justified with the data presented, especially since there is no information on Sr-concentrations for table 1.

We agree. This was poorly worded and not well justified. This now reads: 'More work will be needed to determine if this sample can be a Sr isotope reference material as well as a secondary U/Pb carbonate reference material.'

Lines 214-215: "We hypothesize that U(IV) is complexed with some oxyanion in the lake water (phosphate, bicarbonate, etc) that keeps it in solution and perhaps is also incorporated into the calcite lattice." here it would be good to show some thermody-namic modelling or properties of U(IV)-bearing solutions from the laboratory, there are some of those available in the literature. and perhaps also compare to measurement of U-speciation in highly reducing waters at Forsmark, Sweden (Tullborg et al., 2017, https://www.sciencedirect.com/science/article/pii/S187852201630145X) that show that U is indeed complexed with carbonate in these solution, but is still U(VI) dominated uranyl-complexes. So the explanation presented here may be a bit oversimplified with-out further evidence.

The question of U complexation in a fluid and how it becomes part of the carbonate are unquestionably important and remain to be answered. We added a reference to Langmuir because that is foundational work on the fluid side of things and we included this Tullborg ref as an example of a field situation with highly reduced waters and U is still in solution as U(VI). The question then becomes how that is incorporated into the carbonate as U(IV) and this remains to be answered. Thus we scaled back on our interpretations and offered some suggestions for the way forward.

'While it is easy to conceive of a stratified lake with reducing bottom waters, reduced U is insoluble in most solutions, begging the question of how it is available to go into the calcite \citep{langmuir_uranium_1978}. Elevated actinide concentrations are found in the Great Basin lakes, and it is thought that the carbonate alkalinity is responsible for this elevation \citep{anderson_elevated_1982, simpson_radionuclides_1982}. Similarly, \citet{tullborg_occurrences_2017} demonstrates U(VI) complexes in extremely reducing fluids of deep groundwaters in Sweden. It seems clear that there is a kinetic barrier to U reduction even in the most reducing fluids, and yet some carbonates have entirely reduced U in their structures \citep{sturchio_tetravalent_1998}. More work is needed to understand the incorporation mechanism and use of synchrotron facilities to image the distribution of U with respect to other elements, and XAS measurements of U and other redox sensitive elements are important tools for advancing this research. Additionally lab directed studies that can produce U(IV) in carbonates would be a huge leap forward.'

Line 267; "...this sample could be a standard U/Pb dating, Sr isotopes, and synchrotron U spectroscopy" this sample looks promising as Sr isotope standard. But a few more samples than 2 (although with two aliquots each?) would be needed to confirm this further.

There are three aliquots, but we agree, we are presenting it as a possibility to be worked on by a number of labs before it could possibly be put out there as a reference material. This now reads:

87Sr/86Sr of three aliquots of the Turkana dolomite from the outside (oldest) to the inside (youngest) are indistinguishable from each other at 0.703306 (Table \ref{tab:TBW_Sr}). With the well behaved U/Pb systematics, high concentrations of reduced U and homogeneous 87Sr/86Sr, and further work in collaboration with other labs, this sample could be a reference material for U/Pb dating, Sr isotopes, and synchrotron U spectroscopy.

Summary: line 272: "Details such as the U oxidation state..." Here, and elsewhere, much emphasis is put on the importance of knowing the U oxidation state of the car-bonate for U/Pb dating. How exactly is this affecting the geochronology considerations and outcome? I may have missed it in the MS. please add some discussion about this particular matter

We addressed this in the first instance by saying that there is no indication that the oxidation state of U matters for the reliability of dating.

Associate Editor Comments

Associate Editor Decision: Publish subject to minor revisions (further review by editor) (16 Nov 2020)
by Nick Roberts
Comments to the Author:
Thank you for trying to address the concerns and comments of the reviewers. Once these have been made in a final version, the manuscript should be ready for publication. Please decide on the final outcome of statements such as further data after Covid restrictions, and make sure editorial things like "??" are removed.

I only have one real concern over the manuscript, and that is how the data and discussion are portrayed.
I find the title slightly misleading, or at least, the paper does not give what I would expect based on this.
i.e. the paper describes a selection of techniques, but these are not ever going to be the most common by any stretch. CL followed by LA trace element mapping will probably become the most common (CL already is).
Therefore this paper does not provide a comprehensive review of sample characterization tools – I know it does not suggest that it should, but I find that the title sort of suggests that.
The title also does not mention the use of case studies to demonstrate the methods.
The mapping Uranium section describes four methods – you could even describe these as four uncommon methods!
Rather than fully reviewing any of the characterization methods, the paper presents three case studies. I would prefer to see a fuller review of these methods with a wider range of case studies, or, given the short length of the paper, that it be recast (i.e. not involving much, but a change in title and some sentences in the intro and summary) as a demonstration of some common (CL) and uncommon (synchotron-based) methods.

We agree with AE Nick Roberts that the manuscript does not review more traditional carbonate petrography. We changed the title to reflect that this manuscript presents case studies based on characterization of U and other elements which builds on traditional approaches.

~~A Sample Characterization Toolkit for Carbonate U-Pb Geochronology~~

Tools for uranium characterization in carbonate samples: Case studies of natural U-Pb geochronology reference materials

E Troy Rasbury[1], Theodore M Present[2], Paul Northrup[1], Ryan V Tappero[3], Antonio Lanzirotti[4], Jennifer M Cole[5], Kathleen M Wooton[1], and Kevin Hatton[1]

[1]Department of Geosciences, FIRST, Stony Brook University, 100 Nichols Rd, Stony Brook, NY 11794, USA
[2]Division of Geological and Planetary Sciences, California Institute of Technology, 307 North Mudd Laboratory, Pasadena, CA 91125, USA
[3]NSLS-II, Brookhaven National Laboratory, Upton NY 11973, USA
[4]Center for Advanced Radiation Sources, Randall, Chicago, IL 60637
[5]Department of Science, West Los Angeles College, Culver City, CA 90230, USA

Correspondence: E. Troy Rasbury (troy.rasbury@stonybrook.edu))

Abstract. Laser ablation U-Pb analyses of carbonate (LAcarb) samples has greatly expanded the potential for U-Pb dating to a variety of carbonate producing settings. Carbonates that were previously considered impossible to date using isotope dilution methods may preserve radiogenic domains that ~~are favorably interrogated when~~can be dated using spatially resolved laser ablation geochronology techniques.

Work is ongoing to identify reference materials and to consider best practices for LAcarb. In this study we apply standard and ~~standard and~~ emerging characterization toolsets on three natural samples with the dual goal of enhancing the study of carbonates and in establishing a new set of ~~precisely~~well characterized natural ~~standards~~reference materials for LAcarb studies. We start with the existing carbonate reference material WC-1 from the Permian Reef Complex of Texas, building on the published description to offer a deeper look at U and ~~fluids.~~associated trace elements. We consider a tufa sample from the Miocene Barstow Formation of the Mojave Block, ~~California, as a possible secondary calcite reference material due to its well-behaved U/Pb systematics. There are currently~~ no natural California, as a possible secondary calcite reference material due to its well-behaved U-Pb systematics. There are currently no natural dolomite standards. We present an unusual dolomite sample with very well-behaved U-Pb systematics from the Miocene of the Turkana Basin of Kenya as a possible dolomite reference material for LAcarb dating. In addition to using XRF

mapping and spectroscopy to better understand U in these natural samples, we have analyzed multiple aliquots of each of them for $^{87}Sr/^{86}Sr$ by TIMS. The Sr isotope compositions are ~~reasonably~~analytically homogeneous ~~in~~ within petrographically-homogeneous regions of all three samples, so ~~that~~ these materials could be used as Sr isotope standards as well. ~~This~~While not part of the current 15 contribution, this combination could streamline ~~split stream~~simultaneous LA analyses of $^{87}Sr/^{86}Sr$ and U~~/~~-Pb geochronology.

~~15~~ 1 Introduction

Carbonates are ubiquitous in the Earth's crust and form from a variety of fluids, often with characteristic isotopic and element ratios (Fig. 1). Carbonate producing fluids in all crustal levels range from oxygenated to reducing, from low salinity to high salinity and from low ~~T~~temperature to high ~~T~~temperature. Fluids evolve as they interact with rocks along their flow paths, adding ~~complexity, but also providing an opportunity to consider these processes in more detail. Carbonates are highly susceptible to diagenesis, particularly when the~~

~~20~~20 complexity, but also providing opportunities to trace these processes with the rock's paragenetic history. Carbonate compositions are highly susceptible to diagenetic alteration, particularly when fluid chemistry and temperature changes~~,~~ ~~bringing them into and out~~ affect the thermodynamic stability of ~~the~~ carbonate ~~stability fields.~~minerals. Mixing of fluids can be particularly corrosive such as seen where seawater and fresh water mix in a carbonate platform, or can be responsible for mineral precipitation~~. Introduction~~ depending on the saturation state of the combined fluids (Runnells, 1969; Wigley and Plummer, 1976). Thus, introduction of fluids with different chemistries through

25 exposure, uplift, or burial can destroy the original carbonate prior to precipitation of a new carbonate or can alter the carbonates visibly or at a microscopic scale. Therefore, an important part of ~~any~~ investigation of carbonates should involve establishing field and petrographic relationships. ~~We assume if you are working~~Standard assessment of field and petrographic relationships between carbonate phases is a prerequisite to developing a detailed rock paragenesis necessary for interpreting the timing and source of depositional and diagenetic fluids interacting with ~~carbonates, that your toolkit already involves establishing~~carbonate rocks. Here, we present tools useful for characterizing the incorporation of radiogenic

~~25 field relationships and careful petrography. You have a context that involves knowing the depositional and diagenetic histories, and our focus here is more on elucidating of the geochemsitry as it relates to the potential for incorporation of U and Pb in carbonates.~~

30 elements–especially uranium, lead, and strontium–into carbonates as a means for relating $^{87}Sr/^{86}Sr$ and U/Pb data to carbonate paragenetic frameworks.

It is widely recognized that carbonates are a proxy for the fluids that formed them. Published studies demonstrate the need for careful characterization of carbonates in order to ~~obtain~~interpret geochemical results in geologically meaningful

~~results~~context, and this same attention to detail is needed to understand U-Pb results. Carbonates have element ratios that are controlled by the composition of the fluid and the partition coefficient (Kd) of the element for the crystal lattice (Banner and Hanson, 1990). Special circumstances are required to have elevated U in calcite because the Kd is less than 0.05 (Reeder et al., 2001; Drysdale et al., 2019; Weremeichik et al., 2017). However, aragonite, which is metastable, does not exclude U. (Reeder et al., 2001) and Kelly et al. (2003) suggested that high U contents in a speleothem calcite (which we use as a U(VI) standard), might have ~~resulted~~been inherited from ~~neomorphism of original~~high concentrations in primary aragonite and preserved during neomorphic inversion to calcite. No experimental studies for U incorporation have been reported for dolomite, but it is unlikely to have a higher affinity for U than calcite as they have the similar structures~~,~~ and there is more of a size mismatch with Mg than Ca. Using modern settings and a laboratory understanding of trace element incorporation, we know that U incorporation ~~is higher in~~follows aragonite > high Mg calcite> calcite (Chung and Swart, 1990; Reeder et al., 2001). Seawater has elevated U/Pb, but carbonates forming from seawater have much lower U/Pb, demonstrating that the structure has a much higher affinity for Pb than U (Shen and Boyle, 1988), at least at seawater composition.

~~1988), at least at seawater composition. A missing component here is that no~~No lab experiments have studied U(IV) incorporation in carbonates~~. There are~~, despite several published examples of natural carbonates with reduced U (Sturchio, 1998; Cole et al., 2004) and an additional example we present ~~one more~~ in this contribution. ~~Clearly more~~Because U(IV) is immobile in most aqueous fluids, carbonate minerals that incorporate U(IV) must represent precipitates from poorly-understood fluid compositions in depositional or diagenetic environments. Recent work ~~is needed to understand how reduced U~~on modern calcite from a deep granite aquifer with reducing fluids is ~~available to go into carbonates.~~suggesting a mechanism for U(IV) transport (Drake et al., 2018). Experimental work at elevated T has shown that U(IV)~~Cl~~$Cl_4$0 is soluble in acid solutions (Timofeev et al., 2018), and high T experiments of U in hydrocarbons indicate that economic concentrations can be produced via transport in hydrocarbons ~~(Migdisov et al., 2017), but how would these processes result in incorporation in carbonates?~~(Migdisov et al., 2017), but how would these processes result in incorporation in carbonates? There is likely more than one mechanism and this is a fruitful avenue for future research both of synthetic and natural carbonate samples. Understanding U incorporation in carbonates is important for a holistic approach to U-Pb dating, but there is no evidence that the oxidation state of U in carbonates has any control on the reliability of the dating. However, understanding U speciation might elucidate the depositional or diagenetic condition under which the U was incorporated, and therefore affect the interpretation of the U/Pb date.

Cement stratigraphy is a powerful approach to establish the relative age relationships of carbonate phases, or paragenesis across a basin. This approach uses relative relationships of cements from the thin section scale and correlation of these

throughout a basin or region (Meyers, 1991, 1974). This field to petrographic approach has been used to select samples for geochemistry, providing fundamental insights into the fluid evolution of basins and degree of rock/water interaction e.g. ~~(Ban~~ (Banner and Hanson, 1990), as well as establishing trace and minor element incorporation trends (e.g., Mn/Fe) useful for tracking burial histories (Barnaby and Rimstidt, 1989). Often, combining microanalytical tools that characterize carbonates at the micron to centimeter scale of cement growth zones is required to understand the origin and timing of various textures in complex

~~ner et al., 1988), as well as establishing normal trends in Mn/Fe with burial (Barnaby and Rimstidt, 1989). U-Pb dating in this larger~~ samples. Chemical imaging techniques, carbonate staining, and polarized light, fluorescence, electron, and cathodoluminescence microscopy provide spatial context for quantitative microscale analyses of fluid inclusion, ion microprobe, electron microprobe, and laser ablation measurements. Integrated data from such a toolkit enables collection of LA-U-Pb isochrons that reliably dates a single paragenetic event and permits geologically meaningful interpretation of U-Pb ages. U-Pb dating in this context places age constraints on the fluids which can then be tied to testable hypothesis about the origin and changes in the

fluids whatever the technique for dating is (Lawson et al., 2018; Quade et al., 2017; Parrish et al., 2019; Pisapia et al., 2018; Woodhead et al., 2010; Winter and Johnson, 1995; Hoff et al., 1995; Cole et al., 2005; Polyak et al., 2008, 2013; Luczaj and Goldstein, 2000; Brannon et al., 1996; Godeau et al., 2018; Rasbury et al., 2004, 1997; Pagel et al., 2018; Roberts et al., 2020).

~~Laser ablation mapping (Woodhead et al., 2010, 2007; Piccione et al., 2019; Drost et al., 2018; Roberts et al., 2020), synchrotron XRF mapping (Cole et al., 2004; Piccione et al., 2019; Frisia et al., 2008; Vanghi et al., 2019), PIXE (Ortega et al., 2005, 2003) and µXRF (de Winter et al., 2017) are all ways to take the physical observations of different phases to a new level with in situ chemistry, that maps U in particular, along with other elements that provide details of the fluid chemistry. For the purpose of U-Pb dating, knowledge of mineral lattice location of U and it's oxidation state and speciation provide a fundamen-~~

~~tal~~ 2005, 2003) µXRF (de Winter et al., 2017), and EMPA (Suzuki et al., 2016) permit tying petrographic observations of different phases to in situ chemical maps of U and other elements that inform fluid chemistry. For the purpose of U-Pb dating, knowledge of the mineral lattice location of U and it's oxidation state and speciation provide a fundamental framework for interpreting ages as well as revealing details of the fluid chemistry (Kelly et al., 2006, 2003; Sturchio, 1998; Cole et al., 2004). In some cases, uranium minerals are encapsulated in calcite which can protect them from alteration Suzuki et al. (2016); Ludwig (1978).

~~Cole et al., 2004).~~ Given that the major element composition of seawater has changed appreciably through time (Hardie, 1996; Lowenstein,

2001; Horita et al., 2002), that meteoric fluid compositions are controlled by water rock interaction (Chung and Swart, 1990; Banner and Hanson, 1990) and that deep brines have evolved since deposition in basins (Musgrove and Banner, 1993), we can imagine that there is no such thing as a typical fluid. A holistic approach to dating carbonates should involve an effort to

see back to the fluid or fluids that have been responsible for its formation and how they might have changed through the diagenetic history. This, particularly in the context of how favorable the U concentrations and U/Pb ratios are, will provide an important path towards understanding factors that create favorable carbonate samples for U-Pb dating. The purpose of this contribution is to highlight tools that are available for carbonate characterization relevant to U-Pb dating. These tools build on the more commonly used petrographic approaches, particularly cathodoluminescence (CL) imaging, such as demonstrated in the three case studies presented here.

1.1 Mapping Uranium

While the U/Pb ratio matters for dating, it is usually the U concentration that limits the potential. Mapping U at low concentrations in carbonates is challenging, but necessary to tie U-Pb ages to paragenetic context and to identify datable phases, so the focus here will be on tools that map the distribution of U on the hand specimen to thin section scale.

Fission track mapping (Chung and Swart, 1990; Hoff et al., 1995; Rasbury et al., 2000; Cole et al., 2004; Becker et al., 2002; Wang et al., 1998; Luczaj and Goldstein, 2000; Amiel et al., 1973; Haglund et al., 1969; Gvirtzman et al., 1973) can help to map the distribution of U on the microscopic to hand specimen scales. This simply requires making a polished slab, placing it on a detector such as Lexan plastic (Chung and Swart, 1990) and sending it to a nuclear reactor. Depending on the flux requested, it typically takes weeks for the samples to be returned due to harmful radioactivity produced in the reactor. Once back, the detector has to be etched to increase the size of the tracks for visibility and then a comparison to the rock can be made. Thin sections can be used, making it easier to relate the tracks to the exact phases. There is a modest cost for sending samples to a reactor, but this is an underutilized non-destructive approach. For samples with high U (10's of ppm), modern high resolution scanners can image the tracks. For lower concentration samples, high magnification microscope images can be stitched together to provide a larger scale framework for the U distribution.

Autoradiography (Cole et al., 2003; Pickering et al., 2011) offers the opportunity to examine radioactive elements on the hand specimen scale. Phosphor imaging plates are used in biomedical and biochemical studies to detect samples tagged with radionuclides. While the scanning devices themselves are somewhat costly, phosphor screens can be rented from imaging centers or even purchased at lower cost, making this technique more broadly applicable. Polished hand samples along with a solid standard are left to activate the phosphor over time (days to weeks), ideally in a shielded environment. Following

exposure, the screens are scanned to produce a digital autoradiograph that provides a map of relative differences in U and Th

concentrations directly comparable to the hand specimen (Cole et al., 2003; Pickering et al., 2011). Cm-scale regions of higher U (and Th) can then be targeted further with sampling and other finer-scale mapping techniques.

~~90~~ Synchrotron X-ray fluorescence (SXRF) imaging and X-ray absorption spectroscopy (XAS) techniques have the ability to provide information about both the distribution of major and trace elements, including U and Pb, in samples as well as their valence state and speciation. Using XAS methods it is possible to quantify U valence state at concentrations of a few

ppm. Synchrotron X-ray beamlines are available through a competitive process of general user proposals (Sutton et al., 2002).

These brighter sources offer micron sized resolution for low ppm levels of the elements of interest. Emerging tender energy

~~95~~ spectroscopy (TES~~)~~), using the energy range between soft and hard Xray techniques ~~allow~~allows mapping of elements such as Mg and S that are important in carbonates (Northrup, 2019). In addition to ~~element~~XRF maps which show element distribution and the relationships among elements, spots can be chosen for spectroscopy, providing mineralogy (Mg, Ca) and redox (U, Fe, Mn ~~etc).~~

etc).

Bench-top microscale XRF mapping (µXRF) of major, minor, and trace elements by energy-dispersive spectroscopy permits geochemical characterization of samples at the micron to decimeter scale. X-ray focusing optics, rather than ~~collomation~~collimation, allow

~~100~~ high spatial resolutions (ca. 15-25 µm) with laboratory X-ray sources. µXRF has been used for chemical imagining in diverse fields, including materials characterization, archaeology, and earth sciences (de Winter et al., 2017; Allwood et al., 2018;

Katsuta et al., 2019; Haschke , last; de Winter and Claeys, 2017), and related instruments will be deployed on interplanetary spacecraft (Williford et al., 2018). Qualitative and semi-quantitative imaging and standardless analysis is rapid and versatile, but quantitative composition determination of carbonate rocks is challenging due to the X-ray-transparent carbonate matrix

~~105~~ (de Winter et al., 2017). As shown here, in some samples with high U concentrations, U abundance can be mapped with appropriate analytical conditions, such as incident radiation filtering, multiple beam dwell passes, acquisition under vacuum,

and preparation of thick samples that permit excitation of all available U atoms through the sample depth. Data presented here was acquired using an M4 Tornado (Bruker) operating with a 30 W Rh x-ray tube excited at 50 kV and focused to a 17 µm spot

(1 σ of incident energy at Mo-Kσ) on flat, polished, thick (> 2 mm) samples under 20 mbar vacuum. Fluorescence energy was

detected with two 60 mm^2 XFlash silicon drift detectors (Bruker), energy spectra were deconvolved with Bruker software, and total counts in each emission line region were exported for plotting and visualization using MATLAB (Mathworks).

2 Case Studies

We use three natural carbonates that have potential as LAcarb ~~standards~~reference materials to illustrate imaging and spectroscopy techniques. We also discuss what is known of the geology and geochemistry to provide context for other samples that might be dated.

2.1 Late Permian Marine Cement- Permian Reef Complex

Roberts et al. (2017) offered WC-1 (Walnut Canyon) as a primary standard for LAcarb. This late Permian marine cement sample is reasonably homogeneous with high enough U/Pb and radiogenic enough Pb isotopes to make it a suitable reference material. A brief description of the field relationships and U-Pb characterization were presented in Roberts et al. (2017), but here we expand on this to offer additional insight into the ~~standard~~reference material as well as to highlight characterization techniques that are relevant to any ~~120~~ carbonate study. Similar buildups and cements are described from important oil plays in Kazakhstan

(Dickson and Kenter, 2014), and comparisons have been made to Precambrian marine aragonite cements (Grotzinger and Knoll, 1995). Cements of this type offer good potential for giving ages of penecontemporaneous marine diagenesis.

The Permian Reef Complex, spectacularly exposed in the Guadalupe Mountains National Park of West Texas, stands in relief primarily due to the type of cements that make up WC-1. Neptunian dikes are found parallel to the reef track, filling ~~125~~ fractures that resulted from tensional stresses as the reef built out into the Permian Basin (Hunt et al., 2003; Budd et al., 2013;

Frost et al., 2013). Early marine cements in the reef and within these Neptunian dikes are primarily botryoidal aragonites and are typically a dark brown color. The dark brown color is from organic matter that is occluded in the carbonate such that when broken or sawn these cements smell like hydrocarbons (anecdotally this strong smell is a good criterion for selecting carbonates for dating). The cements have mostly been altered to calcite, though Chafetz et al. (2008) found original aragonite in similar

~~130~~ cements~~.~~ from the same area. Calcite with the greatest alteration is light brown and has less favorable U/Pb (Jones et al., 1995). Petrograpically these cements preserve details of the original fibrous aragonite as inclusion trails. WC-1 (Walnut Canyon) comes from a Neptunian dike in the ~~Tansil Member equivalent of the~~upper Capitan Formation of the Permian Reef Complex, equivalent to the Tansill

Formation on the shelf. This Neptunian dike is exposed in Walnut Canyon just outside the Guadalupe Mountains National Park entrance. The botryoids that fill the Neptunian dike were made of radiating aragonite needles that bundle into cm scale packages. The botryoids grow atop one another from both sides of the dike (Fig. 2). At the hand specimen scale, cross-cutting white veins are obvious ((Fig 3). Other veins are smaller but can be detected with petrography and element mapping (Fig. 43). The Permian Reef Complex has seen many episodes of diagenetic fluids, including meteoric fluids accompanying the Basin and Range extension that exhumed the reef in the Neogene (Bishop et al., 2014; Loyd et al., 2013; Scholle et al., 1992; Budd et al., 2013).

Cathodoluminescence (CL) has been a go-to test for diagenesis, and when an activator such as Mn is present, this often gives phenomenal images that illuminate alteration, as well as veins and single crystals in fractures which can track reactivation and changes in the chemistry and rate of fluid flow. However, it is also understood that Fe quenches luminescence, so the Mn/Fe ratio matters for understanding what luminescence or non-luminescence means (Barnaby and Rimstidt, 1989). In the case of Walnut Canyon, the well preserved botryoids are non-luminescent and cements that line the botryoids are brightly luminescent (Fig. 3). Even through the botryoids are non-luminescent with excellent textural preservation, the wide range of Sr concentrations across the botryoids shows that they have been variably altered (Fig.3, Fig. 4, Fig. 5). Element imaging is complimentary to petrography, and while petrographic techniques like CL can provide qualitative information on Mn and Fe, XRF and LA imaging techniques give quantitative information on the Fe/Mn, Sr/Ca and other ratios and element concentrations, providing far more insight into the carbonate diagenesis. µXRF scanning is reasonably accessible, and we suggest that depending on the original mineralogy, elements like Sr (Fig. 43, Fig. 54) could be mapped and registered so that only the best preserved parts of a rock slab could be targeted for a LAcarb reference material. This should greatly reduce the scatter that is currently seen in the WC-1 reference material.

While optical orientation is preserved and fluid inclusions and aragonite relict mineral inclusions delineate the original acicular growth habit, the carbonate is almost entirely replaced by cloudy brown calcite. This neomorphic replacement may facilitate retention of U (Kelly et al., 2003), or perhaps the organic matter (that gives the sample its color and pungent smell when broken) complexed U and retained it in the calcite. Remarkably, Sr is lost well before U in this system as evidenced by the rather homogeneous U concentration at about 4.5 ppm (which makes this a good U-Pb reference material) and the highly variable Sr (Fig. 43). Isotope dilution of this sample doesn't give much of a spread in U/Pb, so to maximize the spread a range of aliquots from dark brown to light brown were utilized (Roberts et al., 2017). Like the result reported in Jones et al.

(1995), this produced an age that is nominally younger than the age of the reef based on dating of ash beds (Wu et al., 2020) (254 instead of 257 Ma~~),~~, but not outside the uncertainty. The cements postdate reef cementation because they fill fractures, but contain internal sediments and likely cemented penecontemporaneously with reef deposition. The $^{87}Sr/^{86}Sr$ ratios range from 0.7069-0.7072 (Fig. ~~7~~6), with an average of 0.706930~~(69~~(.000069) for samples that make up the bulk of the dike. These values are similar to what Chafetz et al. (2008) reported from samples with primary aragonite from ~~the Tansil equivalent~~peritidal teepee structures ~~from the~~ in the correlative Tansill Formation of the Permian Reef Complex, and are consistent with the Capitanian age of the ~~Tansil~~Tansill reef. Samples at the center of the dike (youngest position) give $^{87}Sr/^{86}Sr$ near 0.7072 (Fig. ~~7~~6). Without more work it is not possible to know if the variation with position from the host is due to diagenesis or if it captures real changes in seawater through the growth of the cements. Rasbury et al. (2004) dated similar cements from the algal mounds of the Laborcita Formation in the Sacramento Mountains of New Mexico, and obtained ages and $^{87}Sr/^{86}Sr$ that ~~was~~were also consistent with the biostratigraphically constrained age of deposition.

Laser ablation maps of WC-1 ~~were~~are presented in Roberts et al. (2017). Sr concentrations ~~ranged~~range up to 7000 ppm, and regions with high Sr have high U. Magnesium is elevated in veins along with V and Mn, as is also shown with µXRF(Fig. ~~5~~4) and TES (Fig. ~~8~~7). While LA and µXRF do not offer the high resolution of synchrotron XRF, they do provide details at the scale that LA dating could be accomplished and few elements are inaccessible with quadrupole mass spectrometers.

High resolution, on the fly (the sample is continually moving and the detector is accumulating counts over a prescribed distance) element mapping in the tender energy range (TES) allows us to examine U, Mg, Sr and S in the Walnut Canyon sample. Comparing U, S, and Sr in a RGB map (Fig. ~~8~~7) illustrates the spotty retention of Sr and S relative to U. As seen in the µXRF images (Fig. 4), Mg is elevated in veins and is thus introduced by later fluids. U(M5) XANES shows that the botryoidal cements have entirely oxidized U (Fig. 8). Uranium concentration in this sample is less than 5 ppm, and the ability to explore ~~As seen in the µXRF images (Fig. 5), Mg is elevated in veins and is thus introduced by later fluids. U(M5) XANES shows that the botryoidal cements have entirely oxidized U (Fig. 9). Uranium concentrations in this samples are less than 5 ppm, and the ability to explore~~ U oxidation states at this concentration is a major advance. An important factor to be considered for exploring for favorable U/Pb in carbonates is how U is incorporated. In the Walnut Canyon case we hypothesize the uranyl was brought to the site of precipitation by an oxidizing fluid (seawater) and structurally incorporated in aragonite which does not exclude U (Reeder et al., 2001; Kelly et al., 2003). Through neomorphism to calcite, U was left behind because active functional groups such as carboxyl have a high affinity for uranyl. Perhaps calcite grew around these complexed U ions preserving near original U concentrations. In contrast, Sr, which is also strongly partitioned into aragonite but has a lower affinity for calcite, was lost to the fluid because it does not have an affinity for organic matter.

2.2 Middle Miocene Tufa- Barstow Formation

The Middle Miocene Barstow Formation crops out in the Rainbow Basin near Barstow California. Tufa mounds are found near the top of the Owl Conglomerate (Cole et al., 2004, 2005) and are assumed to have formed where springs entered a lake similar to Mono and Pyramid Lake tufa towers. These tufa deposits have more than 100 ppm U, several ppm Pb and favorable U/Pb systematics (Cole et al., 2005). Here we build on the work of Cole et al. (2004, 2005) with additional synchrotron imaging, µXRF imaging and spectroscopy techniques. The sample that we are using to illustrate these tools for characterization is large enough to be suitable for distribution as a secondary ~~standard~~reference material for LA carbonate dating (Fig. ~~10~~9). Most of the samples used in the Cole et al. (2005) study were small slabs from Vicki Pedone (Cal State Northridge) and are too small to to distribute beyond our lab. Here, we are characterizing a new sample that is large enough to distribute widely. The previously studied tufa ~~the (Cole et al., 2005) study were small slabs from Vicki Pedone (Cal State Northridge) are too small to to distribute beyond our lab, so we are characterizing a new sample that is large enough to distribute widely. The tufa samples ranged in age from 14.8-17 Ma (Cole et al., 2005). Isotope dilution on this sample is under way and will be completed when Covid quarantine is lifted. However, based on the published ages the sample is approximately 15 Ma, and has $^{238}U/^{206}Pb$ between 150-450.~~ samples ranged in age from 14.8-17 Ma (Cole et al., 2005), so more work will be needed to determine the exact age of this sample.

Becker et al. (2001) showed that layers in the Barstow tufa deposits have a pattern of low (10ppm) to high (several hundred ppm) U concentrations across laminae revealed by fission track mapping. Uranium is lower ~~in~~at the ~~beginning~~base of ~~a~~ laminae where larger crystals of calcite formed, and is higher in micritic calcite which forms the caps of laminae. Becker et al. (2001) reasoned that the laminae reflect seasonal increases in fresh water supply which delivers Ca to a body of water with high alkalinity similar to the Great Basin Lakes. Phosphor imaging shows that in addition to these fine scale trends observed with fission tracks, there are mm to cm scale layers of higher and lower U concentrations (Cole et al., 2004).

~~200~~Synchrotron and µXRF imaging of Sr and Mn faithfully matches the primary layering, demonstrating that later alteration has been minor (Fig. ~~11~~10, Fig. ~~12~~11). A comparison of U-L α maps with and without an incident radiation filter shows that the filter eliminates artifacts that result from scatter in pores, and returns an accurate map of the U (Fig. ~~13~~12). The filtered U µXRF map shows that U is elevated in the micritic areas of the tufa. µXRF maps of Al and Si show that large pores that are

typical of the tufa deposits have clay minerals lining them (Fig. ~~12.~~11). Fe, Cu and Zn are also elevated in the pores. A map of Ba

~~205~~ closely matches the S map suggesting that barite may be present. Strontianite is found in economic abundance in the Barstow Formation (Knopf, 1917). The extremely high Sr concentrations in the tufa calcite (10's of thousands of ppm), suggests these ~~fluids were contributing Sr during deposition. The $^{87}Sr/^{86}Sr$ isotope ratios are similar throughout the sample, with 3 aliquots ranging from 0.719877 to 0.721038 (Table 1). Combining the criteria for selection of aliquots for U/Pb, with high Sr content, is likely to greatly narrow this range, making this a good Sr isotope standard as well as a secondary U/Pb carbonate standard.~~

~~210~~ 235 fluids were contributing Sr during deposition. The $^{87}Sr/^{86}Sr$ isotope ratios of 3 aliquots ranged from 0.719877 to 0.721038 (Table 1). More work will be needed to determine if this sample can be a Sr isotope reference material as well as a secondary U/Pb carbonate reference material.

The U in these tufas is in the reduced state U(IV) as shown by measurements at the L3 edge (Cole et al., 2004), and new data from the M5 edge (Fig. ~~14~~13). With the high U concentration, the Barstow tufa could be a ~~standard~~reference material for U XANES

240 analyses. The Barstow tufa calcite is luminescent throughout (Fig. ~~15~~14), consistent with the occurrence of reduced U in this sample. While it is easy to conceive of a stratified lake with reducing bottom waters, reduced U is insoluble in most solutions~~,~~ (Langmuir, 1978), begging the question of how it is available to go into the calcite. ~~We hypothesize that U(IV) is complexed with some oxyanion in the lake~~

~~215 water (phosphate, bicarbonate, etc) that keeps it in solution and perhaps is also incorporated into the calcite lattice.~~ Elevated actinide concentrations are found in the Great Basin lakes, and it is thought that the carbonate alkalinity is responsible for this elevation (Anderson et al., ~~1982;~~ 1982;~~Simpson et al., 1982).~~ ~~The oxidation state(s) of U in the Mono Lake carbonates is not known, but we imagine waters with similar chemistry might be responsible for elevated U in the Barstow tufa. While we do not have temperatures of formation, the morphology of the tufa is similar to that at Pyramid Lake where warm springs enter the lake~~ 220 ~~(Cole et al., 2004). Perhaps thermal fluids are important for U(IV) mobility.~~

Simpson et al., 1982). Similarly, Tullborg et al. (2017) demonstrates U(VI) complexes in extremely reducing fluids of deep

245 groundwaters in Sweden. It seems clear that there is a kinetic barrier to U reduction even in the most reducing fluids, and yet some carbonates have entirely reduced U in their structures (Sturchio, 1998; Cole et al., 2004). More work is needed to understand the incorporation mechanism and use of synchrotron facilities to image the distribution of U with respect to other elements, and XAS measurements of U and other redox sensitive elements are important tools for advancing this research. Additionally lab directed studies that can produce U(IV) in carbonates would be a huge leap forward.

250 One of the biggest advances in LAcarb dating is a contribution by Drost et al. (2018) which used laser ablation imaging and inspection for concentrations or ratios that reflect something that could be considered to be related (like Sr concentrations). Pooling of pixels based on this criteria from across the mapped region and binning based on some additional criteria like $^{235}U/^{207}Pb$ gives isochron plots with range of values that is typically greater than, and certainly more filled in than, would be

obtained by spot analyses. The approach is justified because it would not be possible to select pixels based on criteria other than the ratios being plotted, that would have a meaningful isochron result if the assumption were invalid. This work built on a monocle approach introduced by Petrus et al. (2017) which provided a visual tool to easily compare maps, ratios, and patterns (such as REE patterns) that can be defined by the user. This package of tools is available in Iolite3 and Iolite4 and, beyond U/Pb dating, offers tremendous potential to better understand relationships between elements and how that relates to deposition and diagenesis. Inspired by the Drost et al. (2018) contribution, we did 45 laser ablation lines on the Barstow tufa (Fig. 16). We used Iolite4 (Paton et al., 2011) for the data reduction. Note the laminae are easily visible in the element maps 16. While the U concentration is not as high in the sparry calcite layers, the U/Th and $^{238}U/^{206}Pb$ ratios are much higher than the micritic calcite 16. Similarly, the $^{208}Pb/^{206}Pb$ and $^{207}Pb/^{206}Pb$ are much lower, showing the radiogenic ingrowth of ^{206}Pb. Sr and Mg concentrations are elevated in the sparry calcite so µXRF maps of slabs would provide a framework for selection of spots for LAcarb (Fig. 12). We extracted pixels based on the criteria that they were greater than 12,500 ppm Sr. We used this value based on the monocle feature in Iolite4 which allowed us to see that this would eliminate most of the pixels outside the sparry calcite (Fig. 17). Nearly 7000 pixels meet the criteria for being greater than 12,500 ppm Sr and less than 1 ppm ^{208}Pb. These were subdivided into 90 bins of 70-80 pixels each based on probability of the $^{207}Pb/^{235}U$ ratio e.g. (Drost et al., 2018). When all of the bins are plotted in Isoplot (Ludwig, 2003), there are tails on the low and high ends of the line. Removing 10% on each end produces a much better line (Fig. 17). The age of 12 Ma is about 20% too young. We did not make a correction because we do not know the age of this sample, but a correction could be made based on the secondary standard reference material and applied to unknowns. The purpose here is not to provide the age, but to show that the sample is very well behaved. Pre-screening with µXRF to establish the best regions to use for LAcarb should produce a reproducible secondary standard reference material for QA/QC.

2.3 Middle Miocene Dolomite

A Miocene conglomerate horizon in the Napenagila fossil locality of the Turkana Basin in Kenya is extensively cemented by calcite and dolomite. The dolomite is unique in a number of ways. It forms an isopachous layer on surfaces of fossil trees, showing that it formed in the saturated zone. It has a bladed habit, and is a bright yellow color, becoming darker yellow in

the growth direction (Fig. ~~18~~17). While only an outer crust of the sample has typical bright orange luminescence, the sample glows in the luminescope (Fig. ~~18~~17). The dolomite has variable trace element concentrations along the growth direction, and

extreme U enrichment in the final phases of growth as shown by synchrotron XRF element mapping (Fig. ~~19~~18), µXRF (Fig. ~~20~~19) and laser ablation (Fig. ~~21~~20). The bladed morphology of the dolomite crystals is strongly emphasized by trace element patterns in the youngest part of the dolomite, and is particularly striking in the very high resolution maps from TES (Fig. ~~19~~18). U M5 XANES shows that the U in the dolomite is in the reduced state (Fig. ~~23~~22). The stratigraphic context of this dolomite and other carbonates from the Turkana Basin is being studied by Kevin Hatton and will be presented in a more comprehensive way elsewhere. Meanwhile, the very well-behaved U-Pb systematics make this a possible dolomite reference material, and the

~~elsewhere. Meanwhile, the very well-behaved U-Pb systematics make this a possible dolomite standard, and the~~ XRF mapping and X-ray spectroscopy make it a good example for carbonate characterization. The $^{238}U/^{206}Pb$ ratios for the dolomite sample range from 250-550. Using a selection criteria of Sr concentrations greater than 2500 ppm, and ^{208}Pb less than 0.3 ppm produces over 2200 pixels. Binning the pixels into 70 bins produces an age of 15 Ma (Fig. ~~22~~21). Removing the 'tails' produces

data that ~~plots~~plot near the concordia curve but ~~is~~are poorly anchored on the common Pb side (Fig. ~~22~~21), and we chose not to assume

an initial isotope value. The average of the $^{206}Pb/^{238}U$ ages produced by selection of pixels within polygons on the basis of high U along a crystal is 14.52 Ma (Fig. ~~22~~21). The average of the $^{206}Pb/^{238}U$ ages based on binning pixels where Sr is greater than 2500 and ^{208}Pb is less than 0.3 ppm (which was based on the monocle inspector in Iolite4) is 14.77 Ma (Fig. ~~22~~21). We are working on isotope dilution of this sample which will provide an age for comparison, but whether the age is correct or not, the U/Pb systematics are very favorable.

~~$^{87}Sr/^{86}Sr$ of the~~three aliquots of the Turkana dolomite from the outside (oldest) to the inside (youngest) are indistinguishable from each other at 0.703306 (Table 2). With the well behaved U/Pb systematics, high concentrations of reduced U and homogeneous $^{87}Sr/^{86}Sr$, and further work in collaboration with other labs, this sample could be a ~~standard~~reference material for U/Pb dating, Sr isotopes, and synchrotron U spectroscopy.

3 Summary

Field relationships and petrography allow us to consider the relative timing of carbonate precipitation and alteration, and the ~~tools~~ tools for demonstrating these relationships are an important first step to any study. XRF mapping (both µXRF and synchrotron XRF) and laser ablation mapping allows us to establish domains within rocks that are time-equivalent and to

work out details of the fluids that were responsible for carbonate precipitation. Details such as the U oxidation state~~,~~ and relationships to other elements helps to further constrain the fluids that have produced the final product. While the U oxidation state does not appear to matter for the reliability of U-Pb ages, a general pattern of elevated U is ~~not necessary~~emerging for ~~U/Pb dating,~~ samples ~~that are amenable to~~with reduced U. While elevated U is not necessary for U-Pb dating, samples that are amenable to LA Carb dating typically must have ppm levels of U. The tools we have described here allow us to provide a spatial context ~~275~~ that with well established petrography and field relationships are foundational for putting U~~/~~-Pb ages into the overall geologic context.

Author contributions. ETR led the effort to review the literature on carbonate characterization. TP did the µXRF imaging of the carbonate standard materials. PN RT, and AL led the efforts for the synchrotron XRF and XANES measurements. KW and KH led the laser ablation mapping efforts. KW did the Sr isotope analyses. JMC did the work on the Barstow tufa. All of the authors contributed to writing the ~~manuscript.~~ manuscript.~~280~~

Competing interests. We declare that there are no competing interests.

Acknowledgements. Portions of this work were performed at beamline X26A of the National Synchrotron Light Source (NSLS), Brookhaven National Laboratory. X26A was supported by the Department of Energy (DOE) - Geosciences (DE-FG02-92ER14244 to The University of Chicago - CARS). Use of the NSLS was supported by DOE under Contract No. DE-AC02-98CH10886. Portions of this research were also performed at the Tender Energy Spectroscopy (TES), X-ray Fluorescence Microprobe (XFM), and Submicron Resolution X-ray ~~Spec-troscopy~~Spectroscopy (SRX) beamlines and used resources of the National Synchrotron Light Source II, a U.S. Department of Energy (DOE) Office of Science User Facility operated for the DOE Office of Science by Brookhaven National Laboratory under Contract No. DE-SC0012704.

Construction of, and work at the TES Beamline was partly funded by the National Science Foundation, Earth Sciences (EAR-1128957), NASA (NNX13AD12G) and the Department of Energy, Geosciences (DE-FG02-12ER16342). µXRF data was acquired in the Caltech GPS Division Analytical Facility with the support of Chi Ma, John Grotzinger, and the Simons Foundation. We thank Stephen Cox, Frank Sousa, Elena Steponaitis and Sidney Hemming for the discovery of the dolomite in the Turkana Basin and acknowledge funding from the Columbia University Global Center for field work. Numerous discussions with Bruce Ward have greatly improved our understanding of carbonates.

Journal reviewers Don Davis and an anonymous reviewer as well as associate editor Nick Roberts are thanked for their thoughtful comments which help improve the clarity of the manuscript.

References

Allwood, A. C., Rosing, M. T., Flannery, D. T., Hurowitz, J. A., and Heirwegh, C. M.: Reassessing evidence of life in 3,700-million-year-old rocks of Greenland, Nature, 563, 241–244, https://doi.org/10.1038/s41586-018-0610-4, http://www.nature.com/articles/ ~~s41586-018-0610-4,~~s41586-018-0610-4, 2018.

Amiel, A. J., Miller, D. S., and Friedman, G. M.: Incorporation of uranium in modern corals, Sedimentology, 20, 523–528, https://doi.org/10.1111/j.1365-3091.1973.tb01629.x, http://doi.wiley.com/10.1111/j.1365-3091.1973.tb01629.x, 1973.

Anderson, R. F., Bacon, M. P., and Brewer, P. G.: Elevated Concentrations of Actinides in Mono Lake, Science, 216, 514–516, https://doi.org/10.1126/science.216.4545.514, https://www.sciencemag.org/lookup/doi/10.1126/science.216.4545.514, 1982.

~~Banner, J., Hanson, G., and Meyers, W.: Rare Earth Element and Nd isotopic variations in regionally extenive dolomites from the BurlingtonKeokuk Formation (Mississippian)- Implications for REE mobility during carbonate diagnesis, Journal of Sedimentary Petrology, 58, 415–432, 1988.~~

Banner, J. L. and Hanson, G. N.: Calculation of simultaneous isotopic and trace element variations during water-rock interaction with applications to carbonate diagenesis, Geochimica et Cosmochimica Acta, 54, 3123–3137, https://doi.org/10.1016/0016-7037(90)90128-8, ~~305~~ https://linkinghub.elsevier.com/retrieve/pii/0016703790901288, 1990.

Barnaby, R. and Rimstidt, J.: Redox conditions of calcite cementation interpreted from Mn-contents and Fe-contents of authigenic calcites, Geological Society of America Bulletin, 101, 795–804, https://doi.org/10.1130/0016-7606(1989)101<0795:RCOCCI>2.3.CO;2, 1989.

Becker, M., Cole, J., Rasbury, E., Pedone, V., Montanez, I., and Hanson, G.: Cyclic variations of uranium concentrations and oxygen isotopes in tufa from the middle Miocene Barstow Formation, Mojave Desert, California, GEOLOGY, 29, 139–142, https://doi.org/10.1130/0091~~310~~7613(2001)029<0139:CVOUCA>2.0.CO;2, 2001.

Becker, M., Rasbury, E., Meyers, W., and Hanson, G.: U–Pb calcite age of the Late Permian Castile Formation, Delaware Basin: a constraint on the age of the Permian–Triassic boundary (?), Earth and Planetary Science Letters, 203, 681–689, https://doi.org/10.1016/S0012821X(02)00877-4, https://linkinghub.elsevier.com/retrieve/pii/S0012821X02008774, 2002.

Bishop, J. W., Osleger, D. A., Montañez, I. P., and Sumner, D. Y.: Meteoric diagenesis and fluid-rock interaction in the Middle Permian Capitan backreef: Yates Formation, Slaughter Canyon, New Mexico, AAPG Bulletin, 98, 1495–1519, https://doi.org/10.1306/05201311158, ~~315~~ http://search.datapages.com/data/doi/10.1306/05201311158, 2014.

Brannon, J. C., Cole, S. C., Podosek, F. A., Ragan, V. M., Coveney, R. M., Wallace, M. W., and Bradley, A. J.: Th-Pb and U-Pb Dating of OreStage Calcite and Paleozoic Fluid Flow, Science, 271, 491–493, https://doi.org/10.1126/science.271.5248.491, https://www.sciencemag.org/lookup/doi/10.1126/science.271.5248.491, 1996.

~~320~~ Budd, D. A., Frost, E. L., Huntington, K. W., and Allwardt, P. F.: Syndepositional Deformation Features In High-Relief Carbonate Platforms: Long-Lived Conduits for Diagenetic Fluids, Journal of Sedimentary Research, 83, 12–36, https://doi.org/10.2110/jsr.2013.3, https://pubs. geoscienceworld.org/jsedres/article/83/1/12-36/145369, 2013.

Chafetz, H. S., Wu, Z., Lapen, T. J., and Milliken, K. L.: Geochemistry of Preserved Permian Aragonitic Cements in the ~~Tepees~~Te-

pees of the Guadalupe Mountains, West Texas and New Mexico, U.S.A., Journal of Sedimentary Research, 78, 187–198, https://doi.org/10.2110/jsr.2008.025, https://pubs.geoscienceworld.org/jsedres/article/78/3/187-198/145192, 2008.

Chung, G. and Swart, P.: The concentration of uranium in fresh-water vadose and phreatic cements in a Holocene ooid cay- A method of identifying ancient water tables, Journal of Sedimentary Petrology, 60, 735–746, 1990.

Cole, J. M., Nienstedt, J., Spataro, G., Rasbury, E., Lanzirotti, A., Celestian, A. J., Nilsson, M., and Hanson, G. N.: Phosphor ~~imaging~~imaging as a tool for in situ mapping of ppm levels of uranium and thorium in rocks and minerals, Chemical Geology, 193, 127–136, ~~330~~ https://doi.org/10.1016/S0009-2541(02)00223-1, https://linkinghub.elsevier.com/retrieve/pii/S0009254102002231, 2003.

Cole, J. M., Rasbury, E. T., Montañez, I. P., Pedone, V. A., Lanzirotti, A., and Hanson, G. N.: Petrographic and trace element analysis of uranium-rich tufa calcite, middle Miocene Barstow Formation, California, USA: Uranium-rich tufa deposits, California, Sedimentology, 51, 433–453, https://doi.org/10.1111/j.1365-3091.2004.00631.x, http://doi.wiley.com/10.1111/j.1365-3091.2004.00631.x, 2004.

Cole, J. M., Rasbury, E. T., Hanson, G. N., Montañez, I. P., and Pedone, V. A.: Using U-Pb ages of Miocene tufa for correlation in a terrestrial ~~335~~ succession, Barstow Formation, California, Geological Society of America Bulletin, 117, 276, https://doi.org/10.1130/B25553.1, https://pubs.geoscienceworld.org/gsabulletin/article/117/3-4/276-287/2146, 2005.

de Winter, N. J. and Claeys, P.: Micro X-ray fluorescence (XRF) line scanning on Cretaceous rudist bivalves: A new method for reproducible trace element profiles in bivalve calcite, SEDIMENTOLOGY, 64, 231–251, https://doi.org/10.1111/sed.12299, 2017.

de Winter, N. J., Sinnesael, M., Makarona, C., Vansteenberge, S., and Claeys, P.: Trace element analyses of carbonates using portable ~~340~~ and micro-X-ray fluorescence: performance and optimization of measurement parameters and strategies, Journal of Analytical Atomic Spectrometry, 32, 1211–1223, https://doi.org/10.1039/C6JA00361C, http://xlink.rsc.org/?DOI=C6JA00361C, 2017.

Dickson, J. A. D. and Kenter, J. A. M.: Diagenetic Evolution of Selected Parasequences Across A Carbonate Platform: Late Paleozoic, Tengiz Reservoir, Kazakhstan, Journal of Sedimentary Research, 84, 664–693, https://doi.org/10.2110/jsr.2014.54, https://pubs.geoscienceworld. ~~org/jsedres/article/84/8/664-693/145419, 2014.~~

~~345~~ 375 org/jsedres/article/84/8/664-693/145419, 2014.

Drake, H., Mathurin, F. A., Zack, T., Schaefer, T., Roberts, N. M. W., Whitehouse, M., Karlsson, A., Broman, C., and Astrom, M. E.: Incorporation of Metals into Calcite in a Deep Anoxic Granite Aquifer, ENVIRONMENTAL SCIENCE & TECHNOLOGY, 52, 493–502, https://doi.org/10.1021/acs.est.7b05258, 2018.

Drost, K., Chew, D., Petrus, J. A., Scholze, F., Woodhead, J. D., Schneider, J. W., and Harper, D. A. T.: An Image Mapping Approach to U-Pb LA-ICP-MS Carbonate Dating and Applications to Direct Dating of Carbonate Sedimentation, Geochemistry, Geophysics, Geosystems, 19, 4631–4648, https://doi.org/10.1029/2018GC007850, http://doi.wiley.com/10.1029/2018GC007850, 2018.

Drysdale, R. N., Zanchetta, G., Baneschi, I., Guidi, M., Isola, I., Couchoud, I., Piccini, L., Greig, A., Wong, H., Woodhead, J. D., Regattieri, E., Corrick, E., Paul, B., Spötl, C., Denson, E., Gordon, J., Jaillet, S., Dux, F., and Hellstrom, J. C.: Partitioning of Mg, Sr, Ba and U ~~350~~ into a subaqueous calcite speleothem, Geochimica et Cosmochimica Acta, 264, 67–91, https://doi.org/10.1016/j.gca.2019.08.001, https: 385 //linkinghub.elsevier.com/retrieve/pii/S0016703719304995, 2019.

Frisia, S., Borsato, A., and Susini, J.: Synchrotron radiation applications to past volcanism archived in speleothems: An overview, Journal of Volcanology and Geothermal Research, 177, 96–100, https://doi.org/10.1016/j.jvolgeores.2007.11.010, https://linkinghub.elsevier.com/retrieve/pii/S0377027307003794, 2008.

Frost, E. L., Budd, D. A., and Kerans, C.: Syndepositional Deformation In A High-Relief Carbonate Platform and Its Effect On Early Fluid Flow As Revealed By Dolomite Patterns, Journal of Sedimentary Research, 82, 913–932, https://doi.org/10.2110/jsr.2012.74, https://pubs.geoscienceworld.org/jsedres/article/82/12/913-932/245332, 2013.

Godeau, N., Deschamps, P., Guihou, A., Leonide, P., Tendil, A., Gerdes, A., Hamelin, B., and Girard, J.-P.: U-Pb dating of calcite cement and diagenetic history in microporous carbonate reservoirs: Case of the Urgonian Limestone, France, Geology, 46, 247–250, https://doi.org/10.1130/G39905.1, https://pubs.geoscienceworld.org/gsa/geology/article/46/3/247/526712/UPb-dating-of-calcite-cement-and-diagenetic, 2018.

Grotzinger, J. P. and Knoll, A. H.: Anomalous Carbonate Precipitates: Is the Precambrian the Key to the Permian?, PALAIOS, 10, 578, https://doi.org/10.2307/3515096, https://pubs.geoscienceworld.org/palaios/article/10/6/578-596/114257, 1995.

Gvirtzman, G., Friedman, G., and Miller, D.: Conntrol and distribution of uranium in coral reefs during diagenesis, Journal of Sedimentary Petrology, 43, 985–997, 1973.

Haglund, D., Friedman, G., and Miller, D.: Effect of fresh water redistribution of uranium in carbonate sediments, Journal of Sedimentary Petrology, 39, 1283–&, 1969.

Hardie, L.: Secular variation in seawater chemistry: An explanation for the coupled secular variation in the mineralogies of marine limestones and potash evaporites over the past 600 my, Geology, 24, 279–283, https://doi.org/10.1130/0091-7613(1996)024<0279:SVISCA>2.3.CO;2, 1996.

Haschke (last), M.: Applications., in: In Laboratory Micro-X-Ray Fluorescence Spectroscopy: Instrumentation and Applications, Springer Series in Surface Sciences, pp. 229–341, Cham: Springer International PublishingCham: Springer International Publishing, https://doi.org/10.1007/978-3-319-04864-2_7., 2014.

Hoff, J., Jameson, J., and Hanson, G.: Application of Pb isotopes to the absolute timing of regional exposure events in carbonate rocks- an example from U-rich dolostones from the Wahoo Formation (Pennsylvanian), Prudhoe Bay, Alaska A, Journal of Sedimentary Research Section A -Sedimentary Petrology and Processes, 65, 225–233, 1995.

Horita, J., Zimmermann, H., and Holland, H. D.: Chemical evolution of seawater during the Phanerozoic, Geochimica et Cosmochimica Acta, 66, 3733–3756, https://doi.org/10.1016/S0016-7037(01)00884-5, https://linkinghub.elsevier.com/retrieve/pii/S0016703701008845, 2002.

Hunt, D. W., Fitchen, W. M., and Kosa, E.: Syndepositional deformation of the Permian Capitan reef carbonate platform, Guadalupe Mountains, New Mexico, USA, Sedimentary Geology, 154, 89–126, https://doi.org/10.1016/S0037-0738(02)00104-5, https://linkinghub.elsevier.com/retrieve/pii/S0037073802001045, 2003.

Jones, C., Halliday, A., and Lohmann, K.: The impact of diagenesis on high-precision UPb dating of ancient carbonates: An example from the Late Permian of New Mexico, Earth and Planetary Science Letters, 134, 409–423, https://doi.org/10.1016/0012-821X(95)00128-Y,

https://linkinghub.elsevier.com/retrieve/pii/0012821X9500128Y, https://linkinghub.elsevier.com/retrieve/pii/0012821X9500128Y, 1995.

Katsuta, N., Takano, M., Sano, N., Tani, Y., Ochiai, S., Naito, S., Murakami, T., Niwa, M., and Kawakami, S.: Quantitative micro-X-ray fluorescence scanning spectroscopy of wet sediment based on the X-ray absorption and emission theories: Its application to freshwater lake sedimentary sequences, Sedimentology, 66, 2490–2510, https://doi.org/10.1111/sed.12603, https://onlinelibrary.wiley.com/doi/abs/10.1111/sed.12603, 2019.

Kelly, S. D., Newville, M. G., Cheng, L., Kemner, K. M., Sutton, S. R., Fenter, P., Sturchio, N. C., and Spötl, C.: Uranyl Incorporation in Natural Calcite, Environmental Science & Technology, 37, 1284–1287, https://doi.org/10.1021/es025962f, https://pubs.acs.org/doi/10.1021/es025962f, 2003.

Kelly, S. D., Rasbury, E. T., Chattopadhyay, S., Kropf, A. J., and Kemner, K. M.: Evidence of a Stable Uranyl Site in Ancient Organic-Rich OrganicRich Calcite, Environmental Science & Technology, 40, 2262–2268, https://doi.org/10.1021/es051970v, https://pubs.acs.org/doi/10.1021/es051970v, 2006.

Knopf, A.: Strontianite deposits near Barstow California, Tech. rep., 1917.

Langmuir, D.: Uranium solution-mineral equilibria at low-temperatures with applications to sedimentary ore-deposits U, Geochimica et Cosmochimica Acta, 42, 547–569, https://doi.org/10.1016/0016-7037(78)90001-7, 1978.

Lawson, M., Shenton, B. J., Stolper, D. A., Eiler, J. M., Rasbury, E. T., Becker, T. P., Phillips-Lander, C. M., Buono, A. S., Becker, S. P., Pottorf, R., Gray, G. G., Yurewicz, D., and Gournay, J.: Deciphering the diagenetic history of the El Abra Formation of eastern Mexico using reordered clumped isotope temperatures and U-Pb dating, GEOLOGICAL SOCIETY OF AMERICA BULLETIN, 130, 617–629, https://doi.org/10.1130/B31656.1, 2018.

Lowenstein, T. K.: Oscillations in Phanerozoic Seawater Chemistry: Evidence from Fluid Inclusions, Science, 294, 1086–1088, https://doi.org/10.1126/science.1064280, https://www.sciencemag.org/lookup/doi/10.1126/science.1064280, 2001.

Loyd, S., Dickson, J., Scholle, P., and Tripati, A.: Extensive, uplift-related and non-fault-controlled spar precipitation in the Permian Capitan Formation, Sedimentary Geology, 298, 17–27, https://doi.org/10.1016/j.sedgeo.2013.10.001, https://linkinghub.elsevier.com/retrieve/pii/S0037073813001887, 2013.

Luczaj, J. A. and Goldstein, R. H.: Diagenesis of the Lower Permian Krider Member, Southwest Kansas, U.S.A.: Fluid-Inclusion, U-Pb, and Fission-Track Evidence for Reflux Dolomitization During Latest Permian Time, Journal of Sedimentary Research, 70, 762–773, https://doi.org/10.1306/2DC40936-0E47-11D7-8643000102C1865D, https://pubs.geoscienceworld.org/jsedres/article/70/3/762-773/99155, 2000.

Ludwig, K.: Uranium-daughter migration and U-Pb isotope apparent ages of uranium ores, Shirley Basin, Wyoming, Economic Geology, 73, 29–49, https://doi.org/10.2113/gsecongeo.73.1.29, 1978.

Ludwig, K. R.: ISOPLOT 3.0: a geochronological toolkit for Microsoft Excel Volume: 4, 2003.

Meyers, W.: Carbonate cement stratigraphy of the Lake Valley Formation (Mississippian) Sacramento Mountains, New Mexico, Journal of Sedimentary Petrology, 44, 837–861, 1974.

Meyers, W.: Calcite cement stratigraphy- An overview, in: Luminescence microscopy and spectroscopy: Qualitative and quantitative applications, edited by BARKER, CE and KOPP, OC, vol. 25 of *SEPM Short coure notes*, pp. 133–148, Society Sedimentary Geology, 1991.

Migdisov, A., Guo, X., Williams-Jones, A., Sun, C., Vasyukova, O., Sugiyama, I., Fuchs, S., Pearce, K., and Roback, R.: Hydrocarbons as ore fluids, Geochemical Perspectives Letters, pp. 47–52, https://doi.org/10.7185/geochemlet.1745, http://www.geochemicalperspectivesletters.org/article1745, 2017.

Musgrove, M. and Banner, J. L.: Regional Ground-Water Mixing and the Origin of Saline Fluids: Midcontinent, United States, Science, 259, 1877–1882, https://doi.org/10.1126/science.259.5103.1877, https://www.sciencemag.org/lookup/doi/10.1126/science.259.5103.1877, 1993.

Northrup, P.: The TES beamline (8-BM) at NSLS-II: tender-energy spatially resolved X-ray absorption spectroscopy and X-ray fluorescence imaging, Journal of Synchrotron Radiation, 26, 2064–2074, https://doi.org/10.1107/S1600577519012761, http://scripts.iucr.org/cgi-bin/paper?S1600577519012761, 2019.

Ortega, R., Devès, G., and Maire, R.: Nuclear microprobe analysis of uranium-rich speleothems: Methodological aspects, Nuclear Instruments and Methods in Physics Research Section B: Beam Interactions with Materials and Atoms, 210, 455–458, https://doi.org/10.1016/S0168-583X(03)01075-9, https://linkinghub.elsevier.com/retrieve/pii/S0168583X03010759, 2003.

Ortega, R., Maire, R., Devès, G., and Quinif, Y.: High-resolution mapping of uranium and other trace elements in recrystallized aragonite–calcite speleothems from caves in the Pyrenees (France): Implication for U-series dating, Earth and Planetary Science Letters, 237, 911–923, https://doi.org/10.1016/j.epsl.2005.06.045, https://linkinghub.elsevier.com/retrieve/pii/S0012821X05004243, 2005.

Pagel, M., Bonifacie, M., Schneider, D. A., Gautheron, C., Brigaud, B., Calmels, D., Cros, A., Saint-Bezar, B., Landrein, P., Sutcliffe, C., Davis, D., and Chaduteau, C.: Improving paleohydrological and diagenetic reconstructions in calcite veins and breccia of a sedimentary basin by combining Δ47 temperature, 18Owater and U-Pb age, Chemical Geology, 481, 1–17, https://doi.org/10.1016/j.chemgeo.2017.12.026, https://linkinghub.elsevier.com/retrieve/pii/S0009254117307076, 2018.

Parrish, J. T., Rasbury, E. T., Chan, M. A., and Hasiotis, S. T.: Earliest Jurassic U-Pb ages from carbonate deposits in the Navajo Sandstone, southeastern Utah, USA, Geology, 47, 1015–1019, https://doi.org/10.1130/G46338.1, https://pubs.geoscienceworld.org/gsa/geology/article/47/11/1015/573442/Earliest-Jurassic-UPb-ages-from-carbonate-deposits, 2019.

Paton, C., Hellstrom, J., Paul, B., Woodhead, J., and Hergt, J.: Iolite: Freeware for the visualisation and processing of mass spectrometric data, Journal of Analytical Atomic Spectrometry, 26, 2508, https://doi.org/10.1039/c1ja10172b, http://xlink.rsc.org/?DOI=c1ja10172b, 2011.

Petrus, J. A., Chew, D. M., Leybourne, M. I., and Kamber, B. S.: A new approach to laser-ablation inductively-coupled-plasma mass spectrometry (LA-ICP-MS) using the flexible map interrogation tool 'Monocle', CHEMICAL GEOLOGY, 463, 76–93, https://doi.org/10.1016/j.chemgeo.2017.04.027, 2017.

Piccione, G., Rasbury, E. T., Elliott, B. A., Kyle, J. R., Jaret, S. J., Acerbo, A. S., Lanzirotti, A., Northrup, P., Wooton, K., and Parrish, R. R.: Vein fluorite U-Pb dating demonstrates post–6.2 Ma rare-earth element mobilization associated with Rio Grande rifting, Geosphere, 15, 1958–1972,

https://doi.org/10.1130/GES02139.1, https://pubs.geoscienceworld.org/gsa/geosphere/article/15/6/1958/574972/ 445485 Vein-fluorite-UPb-dating-demonstrates-post62-Ma, 2019.

Pickering, R., Kramers, J. D., Hancox, P. J., de Ruiter, D. J., and Woodhead, J. D.: Contemporary flowstone development links early hominin bearing cave deposits in South Africa, Earth and Planetary Science Letters, 306, 23–32, https://doi.org/10.1016/j.epsl.2011.03.019, https: //linkinghub.elsevier.com/retrieve/pii/S0012821X11001634, 2011.

Pisapia, C., Deschamps, P., Battani, A., Buschaert, S., Guihou, A., Hamelin, B., and Brulhet, J.: U/Pb dating of geodic calcite: new 450490 insights on Western Europe major tectonic events and associated diagenetic fluids, Journal of the Geological Society, 175, 60–70, https://doi.org/10.1144/jgs2017-067, http://jgs.lyellcollection.org/lookup/doi/10.1144/jgs2017-067, 2018.

Polyak, V., Hill, C., and Asmerom, Y.: Age and Evolution of the Grand Canyon Revealed by U-Pb Dating of Water Table-Type Speleothems, Science, 319, 1377–1380, https://doi.org/10.1126/science.1151248, https://www.sciencemag.org/lookup/doi/10.1126/science.1151248, 2008.

455495 Polyak, V., DuChene, H., Davis, D., Palmer, A., Palmer, M., and Asmerom, Y.: Incision history of Glenwood Canyon, Colorado, USA, from the uranium-series analyses of water-table speleothems, International Journal of Speleology, 42, 193–202, https://doi.org/10.5038/1827806X.42.3.3, http://scholarcommons.usf.edu/ijs/vol42/iss3/3/, 2013.

Quade, J., Rasbury, E., Huntington, K., Hudson, A., Vonhof, H., Anchukaitis, K., Betancourt, J., Latorre, C., and Pepper, M.: Isotopic characterization of late Neogene travertine deposits at Barrancas Blancas in the eastern Atacama Desert, Chile, Chemical Geology, 466, 460500 41–56, https://doi.org/10.1016/j.chemgeo.2017.05.004, https://linkinghub.elsevier.com/retrieve/pii/S000925411730270X, 2017.

Rasbury, E., Hanson, G., Meyers, W., and Saller, A.: Dating of the time of sedimentation using UPb ages for paleosol calcite, Geochimica et Cosmochimica Acta, 61, 1525–1529, https://doi.org/10.1016/S0016-7037(97)00043-4, https://linkinghub.elsevier.com/retrieve/pii/S0016703797000434, 1997.

Rasbury, E., Ward, W., Hemming, N., Li, H., Dickson, J., Hanson, G., and Major, R.: Concurrent U–Pb age and seawater 87Sr/86Sr value of a 465505 marine cement, Earth and Planetary Science Letters, 221, 355–371, https://doi.org/10.1016/S0012-821X(04)00105-0, https://linkinghub.elsevier.com/retrieve/pii/S0012821X04001050, 2004.

Rasbury, E. T. and Cole, J. M.: Directly dating geologic events: U-Pb dating of carbonates, Reviews of Geophysics, 47, RG3001, https://doi.org/10.1029/2007RG000246, http://doi.wiley.com/10.1029/2007RG000246, 2009.

Rasbury, E. T., Meyers, W. J., Hanson, G. N., Goldstein, R. H., and Saller, A. H.: Relationship of Uranium to ~~Petrogra-~~ 470 Petrogra510 phy of Caliche Paleosols with Application to Precisely Dating the Time of Sedimentation, Journal of Sedimentary Research, 70, 604–618, https://doi.org/10.1306/2DC4092B-0E47-11D7-8643000102C1865D, https://pubs.geoscienceworld.org/jsedres/article/70/3/604-618/99126, 2000.

Reeder, R. J., Nugent, M., Tait, C., Morris, D. E., Heald, S. M., Beck, K. M., Hess, W. P., and Lanzirotti, A.: Coprecipitation of Uranium(VI) with Calcite: XAFS, micro-XAS, and luminescence characterization, Geochimica et Cosmochimica Acta, 65, 3491–3503, 475515 https://doi.org/10.1016/S0016-7037(01)00647-0, https://linkinghub.elsevier.com/retrieve/pii/S0016703701006470, 2001.

Roberts, N. M. W., Rasbury, E. T., Parrish, R. R., Smith, C. J., Horstwood, M. S. A., and Condon, D. J.: A calcite reference material for LA-ICP-MS U-Pb geochronology: Calcite RM for LA-ICP-MS U-Pb dating, Geochemistry, Geophysics, Geosystems, 18, 2807–2814, https://doi.org/10.1002/2016GC006784, http://doi.wiley.com/10.1002/2016GC006784, 2017.

Roberts, N. M. W., Drost, K., Horstwood, M. S. A., Condon, D. J., Chew, D., Drake, H., Milodowski, A. E., McLean, N. M., Smye, A. J., Walker, R. J., Haslam, R., Hodson, K., Imber, J., Beaudoin, N., and Lee, J. K.: Laser ablation inductively coupled plasma mass spectrometry (LA-ICP-MS) U– Pb carbonate geochronology: strategies, progress, and limitations, Geochronology, 2, 33–61, https://doi.org/10.5194/gchron-2-33-2020, https://www.geochronology.netgchron.copernicus.org/articles/2/33/2020/, 2020.

Runnells, D.: Diagenesis, chemical sediments, and mixing of natural waters, Journal of Sedimentary Petrology, 39, 1188–&, 1969.

S. J. Mazzullo: Calcite Pseudospar Replacive of Marine Acicular Aragonite, and Implications for Aragonite Cement Diagenesis, SEPM Journal of Sedimentary Research, Vol. 50, https://doi.org/10.1306/212F7A18-2B24-11D7-8648000102C1865D, https://pubs.geoscienceworld.org/jsedres/article/50/2/409-422/97298, 1980.

Scholle, P. A., Ulmer, D. S., and Melim, L. A.: Late-stage calcites in the Permian Capitan Formation and its equivalents, Delaware Basin margin, west Texas and New Mexico: evidence for replacement of precursor evaporites, Sedimentology, 39, 207–234, https://doi.org/10.1111/j.1365-3091.1992.tb01035.x, http://doi.wiley.com/10.1111/j.1365-3091.1992.tb01035.x, 1992.

Shen, G. T. and Boyle, E. A.: Determination of lead, cadmium and other trace metals in annually-banded corals, Chemical Geology, 67, 47–62, https://doi.org/10.1016/0009-2541(88)90005-8, https://linkinghub.elsevier.com/retrieve/pii/0009254188900058, 1988.

Simpson, H. J., Trier, R. M., Toggweiler, J. R., Mathieu, G., Deck, B. L., Olsen, C. R., Hammond, D. E., Fuller, C., and Ku, T. L.: Radionuclides in Mono Lake, California, Science, 216, 512–514, https://doi.org/10.1126/science.216.4545.512, https://www.sciencemag.org/lookup/doi/10.1126/science.216.4545.512, 1982.

Sturchio, N. C.: Tetravalent Uranium in Calcite, Science, 281, 971–973, https://doi.org/10.1126/science.281.5379.971, https://www.sciencemag.org/lookup/doi/10.1126/science.281.5379.971, 1998.

Sutton, S. R., Bertsch, P. M., Newville, M., Rivers, M., Lanzirotti, A., and Eng, P.: Microfluorescence and Microtomography Analyses of Heterogeneous Earth and Environmental Materials, Reviews in Mineralogy and Geochemistry, 49, 429–483, https://doi.org/10.2138/rmg.2002.49.8, https://pubs.geoscienceworld.org/rimg/article/49/1/429-483/140753, 2002.

Suzuki, Y., Mukai, H., Ishimura, T., Yokoyama, T. D., Sakata, S., Hirata, T., Iwatsuki, T., and Mizuno, T.: Formation and Geological Sequestration of Uranium Nanoparticles in Deep Granitic Aquifer, Scientific Reports, 6, https://doi.org/10.1038/srep22701, 2016.

Timofeev, A., Migdisov, A. A., Williams-Jones, A. E., Roback, R., Nelson, A. T., and Xu, H.: Uranium transport in acidic brines under reducing conditions, Nature Communications, 9, 1469, https://doi.org/10.1038/s41467-018-03564-7, http://www.nature.com/articles/s41467-018-03564-7, 2018.

Tullborg, E.-L., Suksi, J., Geipel, G., Krall, L., Auqué, L., Gimeno, M., and Puigdomenech, I.: The Occurrences of Ca2UO2(CO3)3 Complex in Fe(II) Containing Deep Groundwater at Forsmark, Eastern Sweden, Procedia Earth and Planetary Science, 17, 440–443, https://doi.org/10.1016/j.proeps.2016.12.111, https://linkinghub.elsevier.com/retrieve/pii/S187852201630145X, 2017.

Vanghi, V., Borsato, A., Frisia, S., Howard, D. L., Gloy, G., Hellstrom, J., and Bajo, P.: High-resolution synchrotron X-ray fluorescence

investigation of calcite coralloid speleothems: Elemental incorporation and their potential as environmental archives, Sedimentology, 66, 2661–2685, https://doi.org/10.1111/sed.12607, https://onlinelibrary.wiley.com/doi/abs/10.1111/sed.12607, 2019.

Wang, Z., Rasbury, E., Hanson, G., and Meyers, W.: Using the U-Pb system of calcretes to date the time of sedimentation of clastic sedimentary rocks, Geochimica et Cosmochimica Acta, 62, 2823–2835, https://doi.org/10.1016/S0016-7037(98)00201-4, https://linkinghub. elsevier.com/retrieve/pii/S0016703798002014, 1998.

Weremeichik, J. M., Gabitov, R. I., Thien, B. M., and Sadekov, A.: The effect of growth rate on uranium partitioning between individual calcite crystals and fluid, Chemical Geology, 450, 145–153, https://doi.org/10.1016/j.chemgeo.2016.12.026, https://linkinghub.elsevier. com/retrieve/pii/S0009254116306866, 2017.

Wigley, T. and Plummer, L.: Mixing of carbonate waters, Geochimica et Cosmochimica Acta, 40, 989–995, https://doi.org/10.1016/00167037(76)90041-7, 1976.

Williford, K. H., Farley, K. A., Stack, K. M., Allwood, A. C., Beaty, D., Beegle, L. W., Bhartia, R., Brown, A. J., de la Torre Juarez, M., Hamran, S.-E., Hecht, M. H., Hurowitz, J. A., Rodriguez-Manfredi, J. A., Maurice, S., Milkovich, S., and Wiens, R. C.: The NASA Mars 2020 Rover Mission and the Search for Extraterrestrial Life, in: From Habitability to Life on Mars, pp. 275–308, Elsevier, https://doi.org/10.1016/B978-0-12-809935-3.00010-4, https://linkinghub.elsevier.com/retrieve/pii/B9780128099353000104, 2018.

Winter, B. L. and Johnson, C. M.: UPb dating of a carbonate subaerial exposure event, Earth and Planetary Science Letters, 131, 177–187, https://doi.org/10.1016/0012-821X(95)00026-9, https://linkinghub.elsevier.com/retrieve/pii/0012821X95000269, 1995.

Woodhead, J., Reisz, R., Fox, D., Drysdale, R., Hellstrom, J., Maas, R., Cheng, H., and Edwards, R. L.: Speleothem climate records from deep time? Exploring the potential with an example from the Permian, Geology, 38, 455–458, https://doi.org/10.1130/G30354.1, http://pubs.geoscienceworld.org/geology/article/38/5/455/130254/Speleothem-climate-records-from-deep-time, 2010.

Woodhead, J. D., Hellstrom, J., Hergt, J. M., Greig, A., and Maas, R.: Isotopic and elemental imaging of geological materials by laser ablation inductively coupled plasma-mass spectrometry, Geostandards and Geoanalytical Research, 31, 331–343, 2007.

Wu, Q., Ramezani, J., Zhang, H., Yuan, D.-x., Erwin, D. H., Henderson, C. M., Lambert, L. L., Zhang, Y.-c., and Shen, S.-z.: High-precision U-Pb zircon age constraints on the Guadalupian in West Texas, USA, Palaeogeography, Palaeoclimatology, Palaeoecology, 548, 109668, https://doi.org/10.1016/j.palaeo.2020.109668, https://linkinghub.elsevier.com/retrieve/pii/S0031018220301139, 2020.

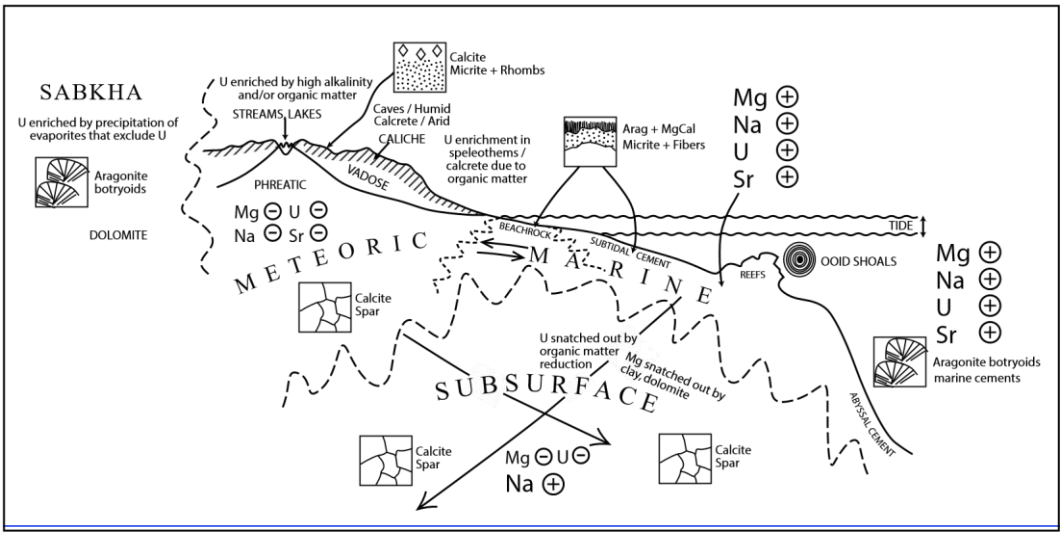
SABKHA
U enriched by precipitation of evaporites that exclude U
Aragonite botryoids
DOLOMITE
U enriched by high alkalinity and/or organic matter
STREAMS, LAKES
Calcite Micrite + Rhombs
Caves / Humid Calcrete / Arid
CALICHE
U enrichment in speleothems / calcrete due to organic matter
PHREATIC
VADOSE
Mg ⊖ U ⊖
Na ⊖ Sr ⊖
METEORIC
Arag + MgCal Micrite + Fibers
Mg ⊕
Na ⊕
U ⊕
Sr ⊕
BEACHROCK
SUBTIDAL CEMENT
TIDE
REEFS
OOID SHOALS
MARINE
Calcite Spar
U snatched out by organic matter reduction
Mg snatched out by clay, dolomite
SUBSURFACE
ABYSSAL CEMENT
Aragonite botryoids marine cements
Calcite Spar
Mg ⊖ U ⊖
Na ⊕
Calcite Spar

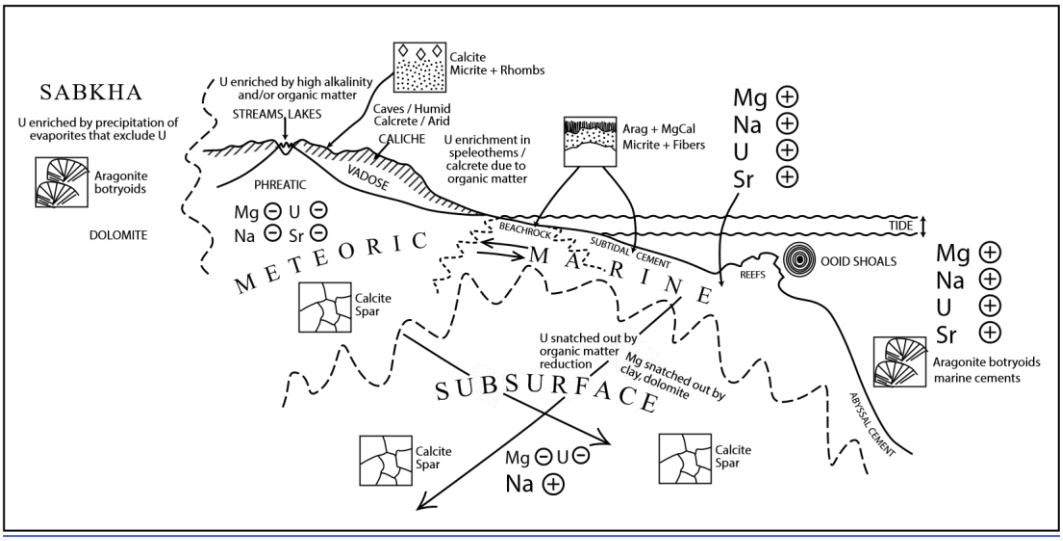
SABKHA
U enriched by precipitation of evaporites that exclude U
Aragonite botryoids
DOLOMITE
U enriched by high alkalinity and/or organic matter
STREAMS, LAKES
Calcite Micrite + Rhombs
Caves / Humid Calcrete / Arid
CALICHE
U enrichment in speleothems / calcrete due to organic matter
PHREATIC
VADOSE
Mg ⊖ U ⊖
Na ⊖ Sr ⊖
METEORIC
Arag + MgCal Micrite + Fibers
Mg ⊕
Na ⊕
U ⊕
Sr ⊕
BEACHROCK
SUBTIDAL CEMENT
TIDE
REEFS
OOID SHOALS
MARINE
Calcite Spar
U snatched out by organic matter reduction
Mg snatched out by clay, dolomite
SUBSURFACE
ABYSSAL CEMENT
Aragonite botryoids marine cements
Calcite Spar
Mg ⊖ U ⊖
Na ⊕
Calcite Spar

Figure 1. Cartoon of the variety of carbonate producing environments with arrows indicating the direction the elements would change through diagenetic alteration (Rasbury and Cole, 2009) We would like to see U concentrations and oxidation states be an important component in understanding fluids and diagenesis

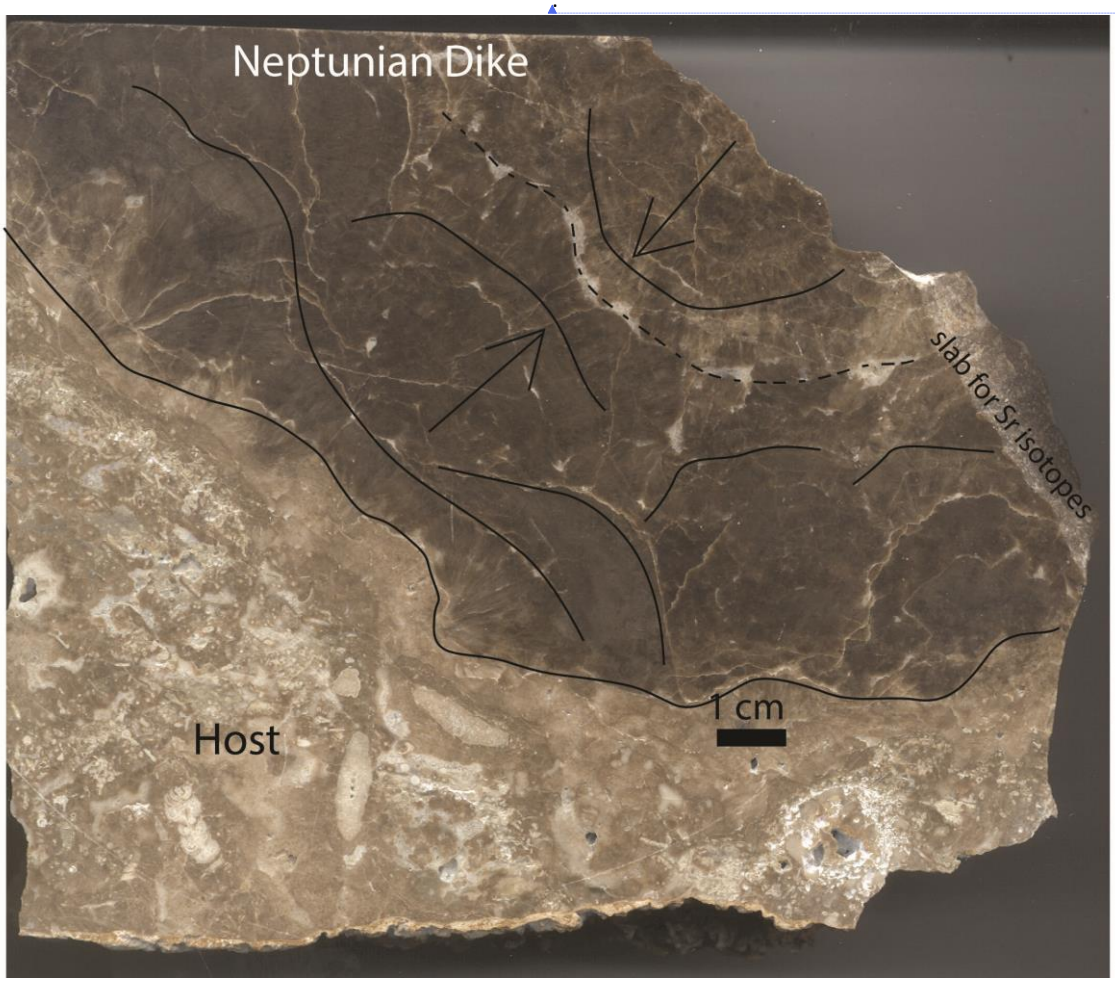

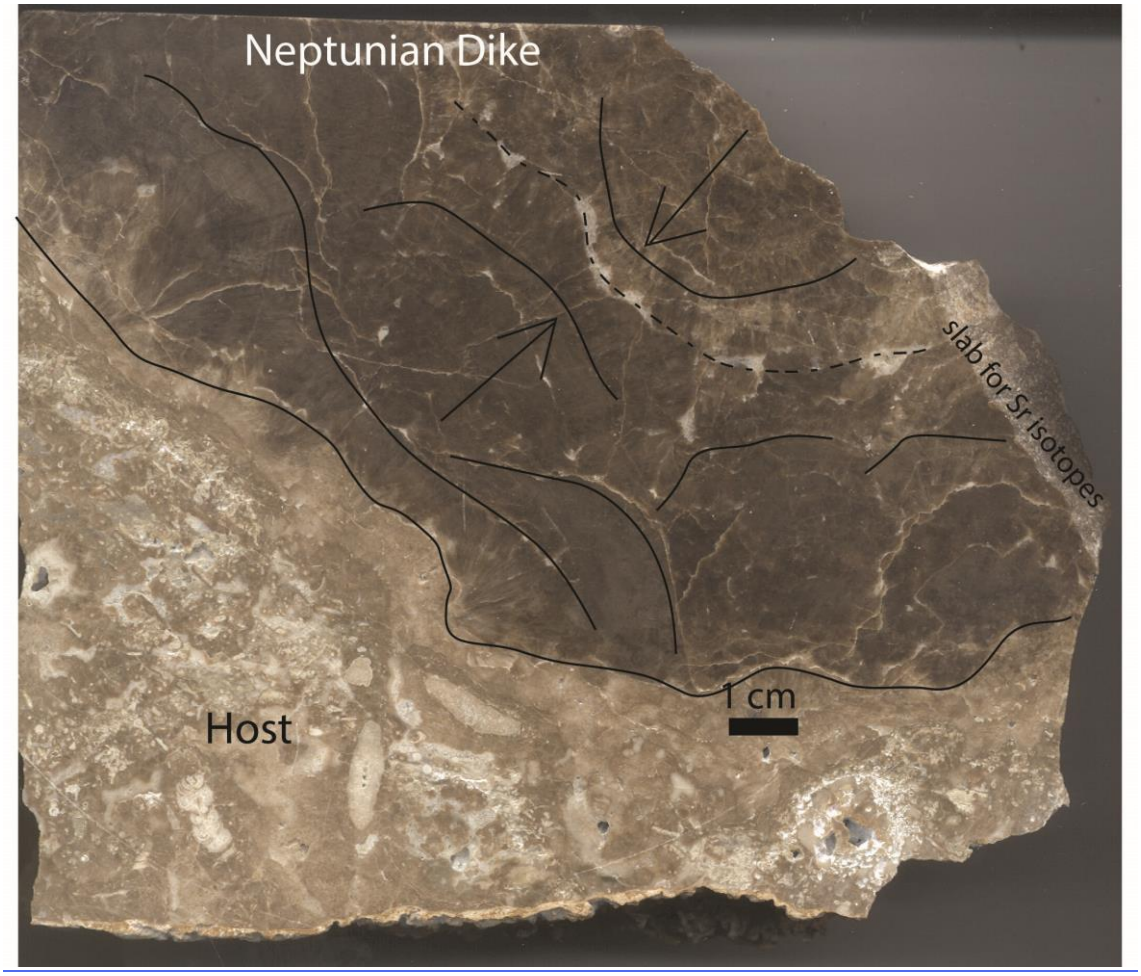

Figure 2. Large hand sample from a Neptunian dike at Walnut Canyon. The lighter brown limestone on the left is the reef rock with abundant large forams visible here. The dark brown botryoids can be seen growing from both sides of this oblique slab through the dike carbonate. Curved lines show approximate botryoid boundaries and arrows point in the growth direction. The dashed line is approximately the center of the dike. A white calcite cement lines many of the botryoids and occurs in the center of the dike. A slab from the host to the center was analyzed for the Sr isotopes presented in this paper.

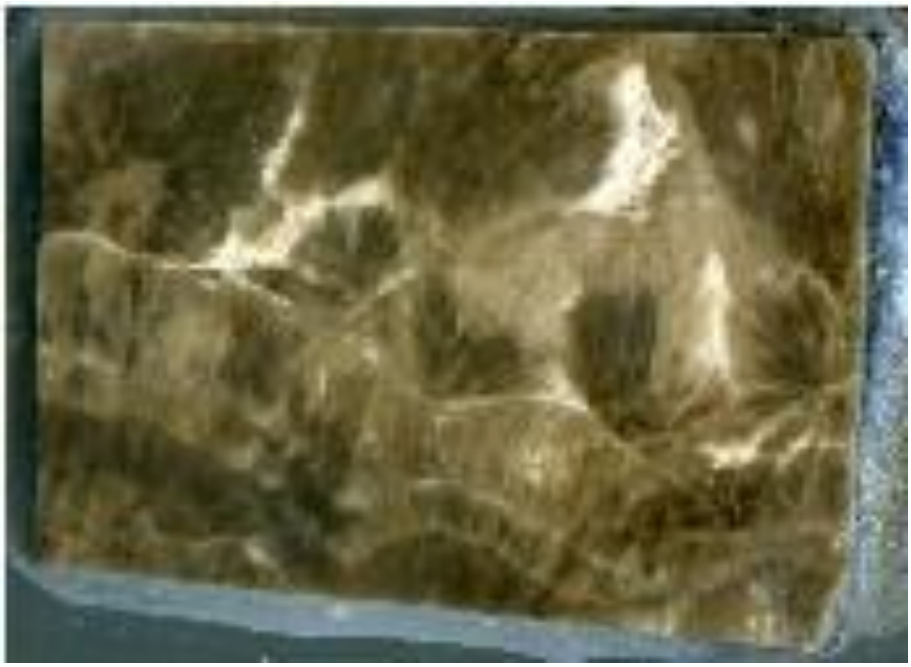

~~Figure 3. Polished slab from the Walnut Canyon Neptunian Dike sample used in this study to illustrate various tools for characterization. This is approximately 3 cm across. This is a similar size to that being distributed a a primary standard (Roberts et al., 2017). Note the variability of color from very dark to light brown, and white veins. The fibrous botyroidal texture is visible even at this scale, and complexities due to veins should be easily avoided when using this as a LAcarb standard.~~

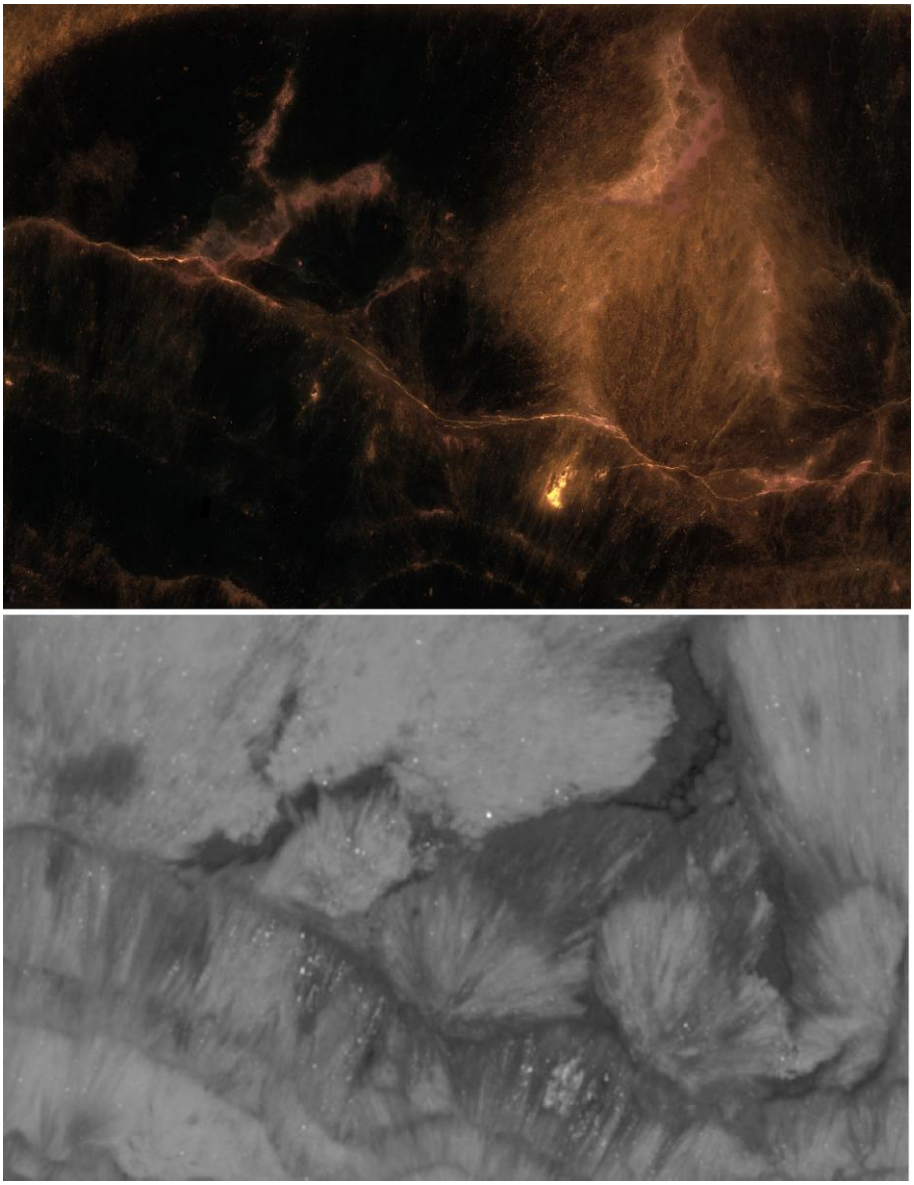

Figure 4. Upper image is a photomosaic of 639 CL photos. The bottom imaage is a microXRF map of Sr (details in the next figure caption). Areas that are brightly luminescent have low Sr. Boundaries between botryoid layers are luminescent (and white so easy to avoid) and should be avoided when using this sample as a standard. This microXRF map of Sr beautifully shos the texture of the sample. We suggest that this easy screening technique could be done on all slabs being used for a LA standard, and that this could greatly reduce the scatter that researchers are finding for this standard.

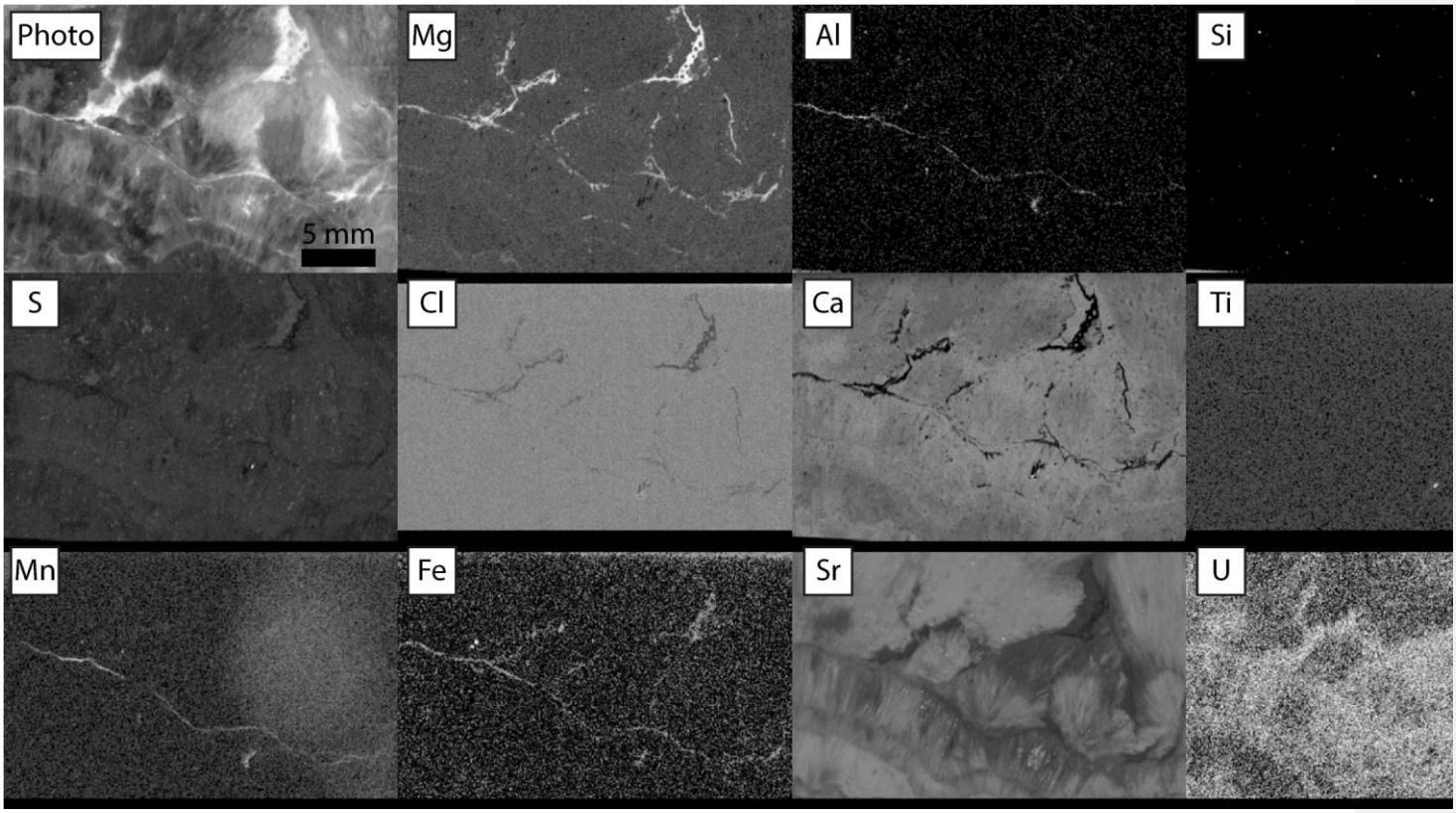
Photo
5 mm
Mg
Al
Si
S
Cl
Ca
Ti
Mn
Fe
Sr
U

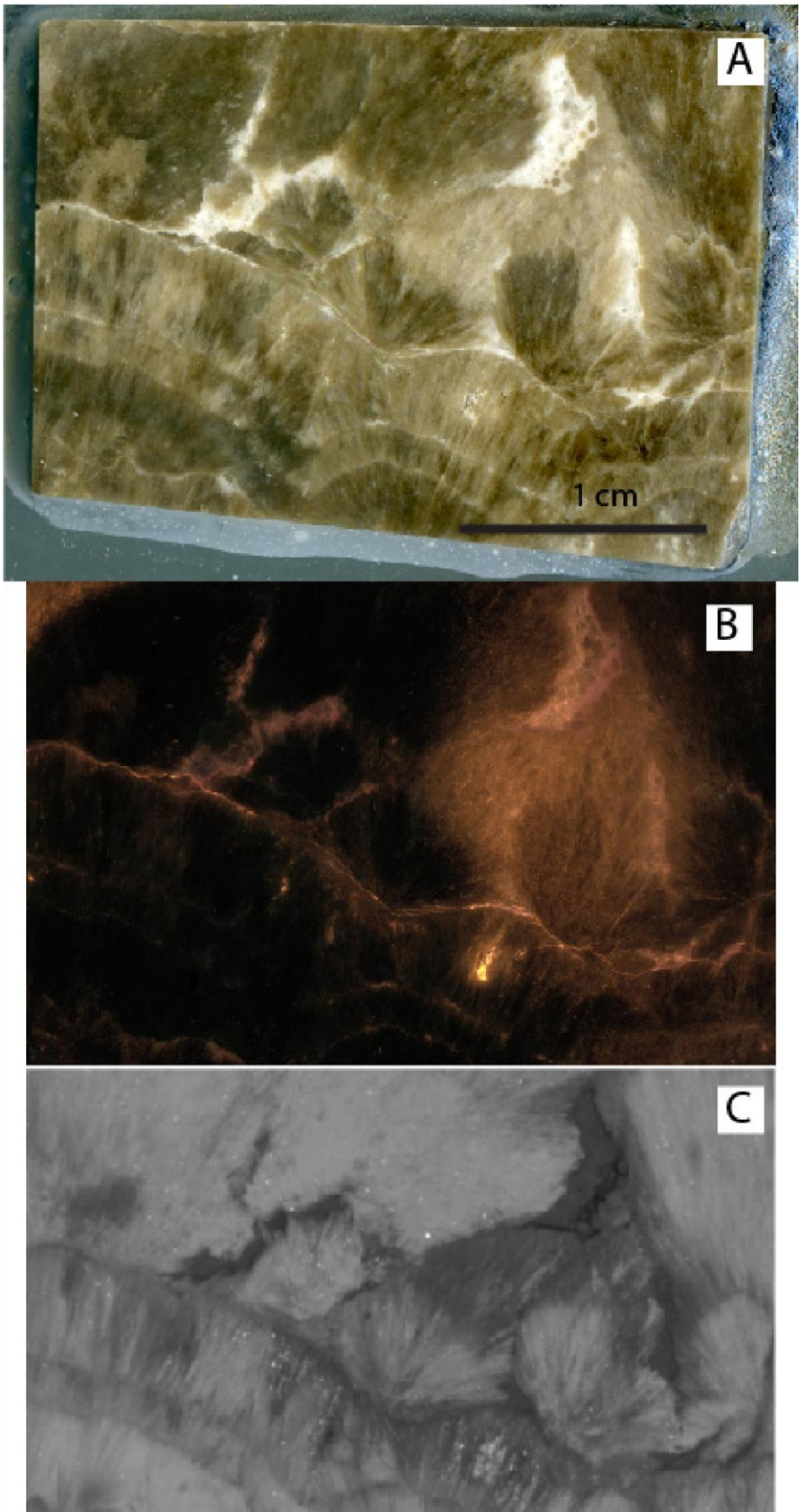
A
1 cm
B
C

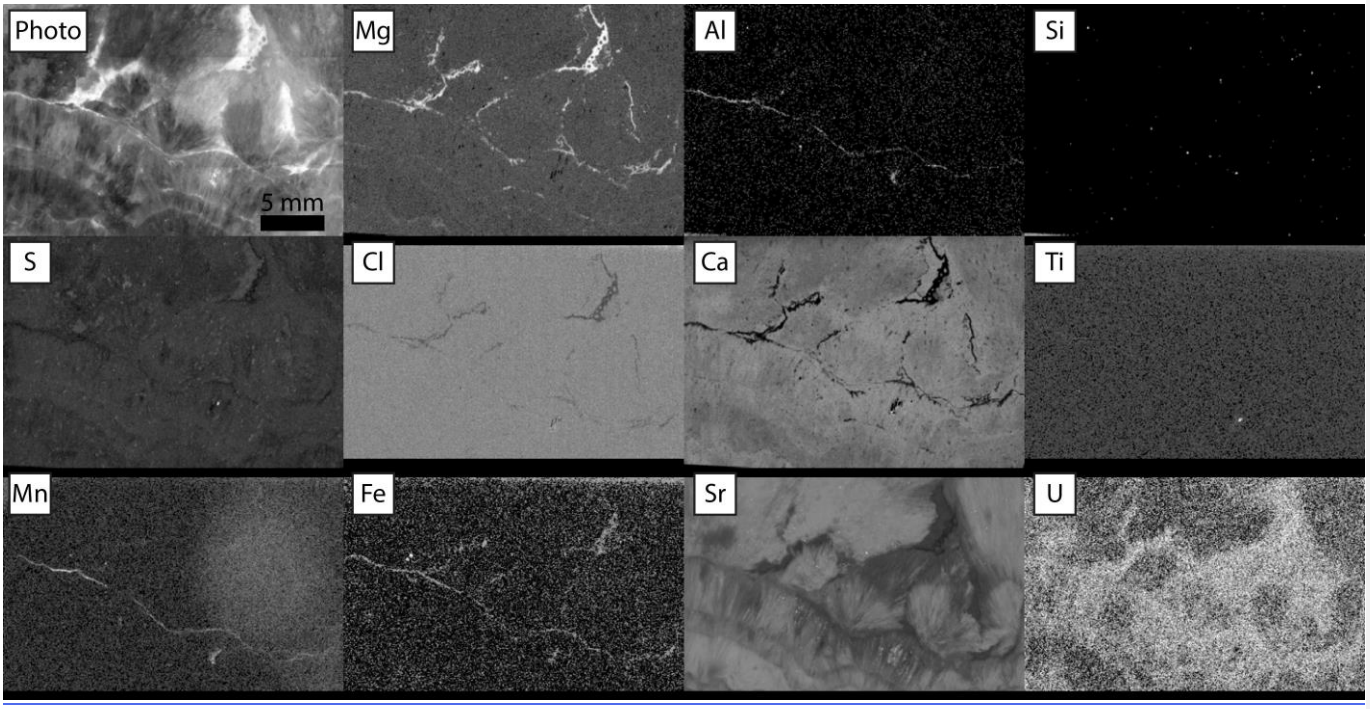

Figure 4. Relative intensities of emission regions for each element detected in Walnut Canyon, imaged at 20 µm pixels with 1.5 s.d. gaussian blur. Dwell time was 30 ms/pixel for maps with no incident radiation filter (Mg, Al, Si, S, Ca). Dwell time was 60 ms/pixel for maps with incident radiation filtered with 100 µm Al, 50 µm Ti, 20 µm Cu foil (Cl, Ti, Mn, Fe, Sr, U). Each panel is gamma and contrast adjusted to emphasize gradients between textures.

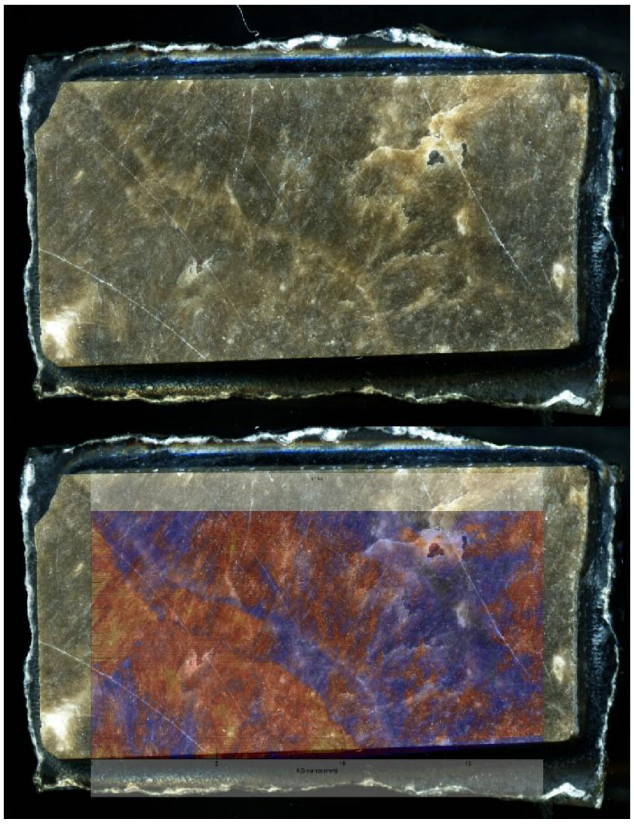

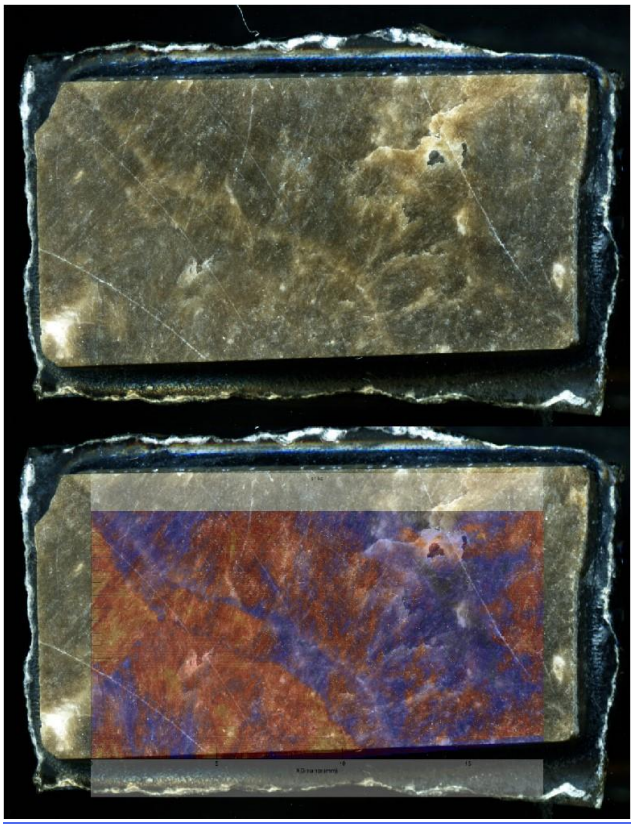

Figure ~~6~~5. Synchrotron XRF Sr maps from beamline X26A NSLS Brookhaven National Lab overlain on the slab that was imaged. This XRF map was accomplished by on the fly scanning. To obtain U maps, we would have had to scan the same area above and below the binding energy for U and make a difference map because the SrKa peak is so large that the shoulder overlaps with the far less abundant UL3 peak. Still, based on the wealth of background information, we know that Sr is lost before U, so that focusing on botryoids with elevated Sr should produce the best areas for LAcarb ~~standardization.~~reference material. This type of image can be registered for laser ablation so that only the most favorable areas are used ~~for standardization~~as a reference material.

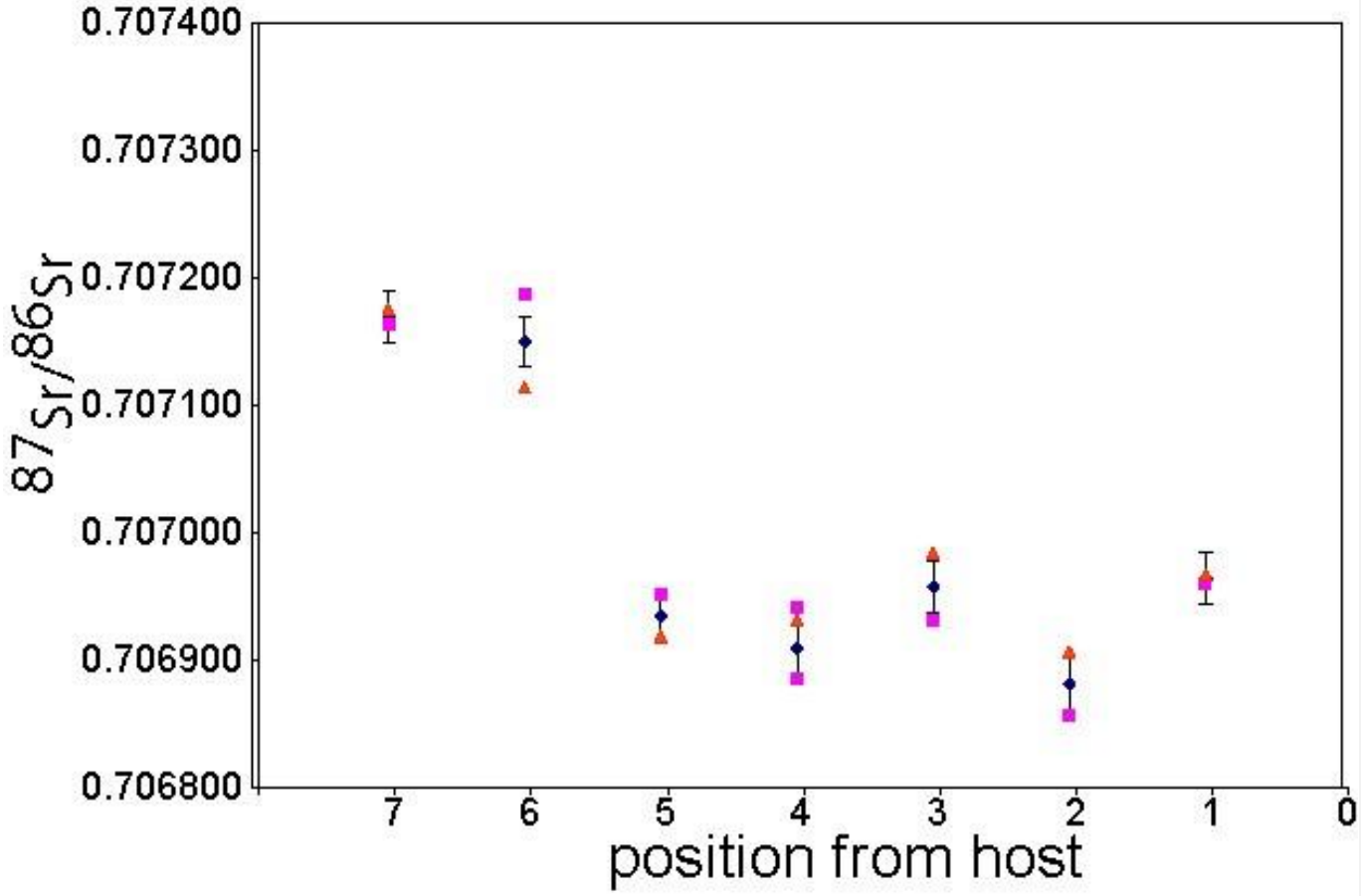
0.707400
0.707300
0.707200
0.707100
0.707000
0.706900
0.706800
87Sr/86Sr
7
6
5
4
3
2
1
0
position from host

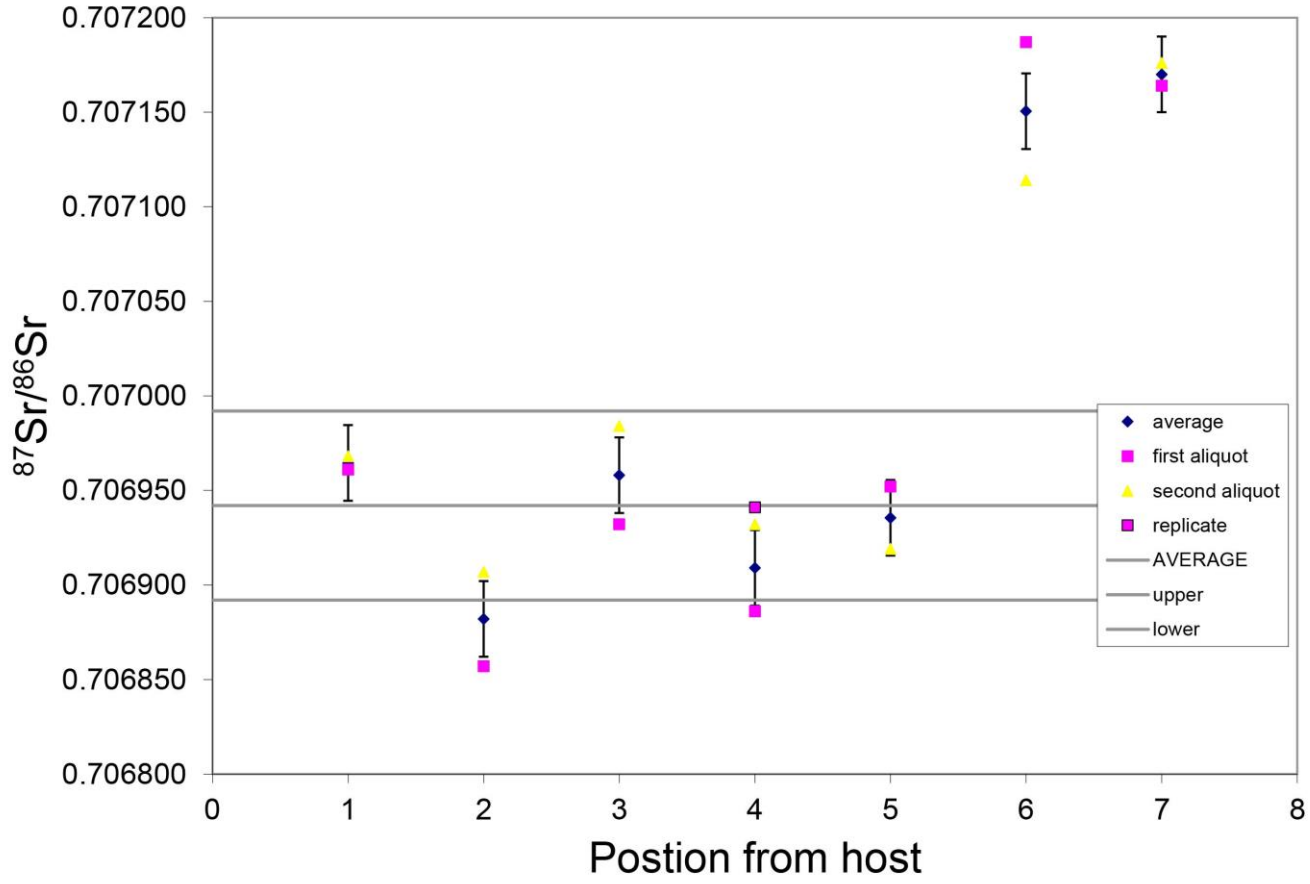

Figure ~~7~~6. This graph shows Sr isotopes from the host to the center of the Neptunian dike. The aliquots were microsampled, dissolved and put through Sr spec resin, and run by Thermal Ionization Mass Spectrometry. The pink symbols represent two independent analyses from slabs that are quasi-equal distance from the host, and the blue is the average of those analyses. While showing variability, the dark brown calcite has $^{87}Sr/^{86}Sr$ like Capitanian seawater with an average of 1-5 of 0.706930(~~69~~0.000069). The samples from positions 6 and 7 are a light brown color and a boundary is clearly visible in 6. These may represent later fluid alteration, or an extended marine cement history. This is presented because we suggest that this sample may also be a useful Sr isotope reference material. The slabs are about 0.5 cm across.

~~This is presented because we suggest that this sample may also be a useful Sr isotope standard. The slabs are about 0.5 cm across.~~

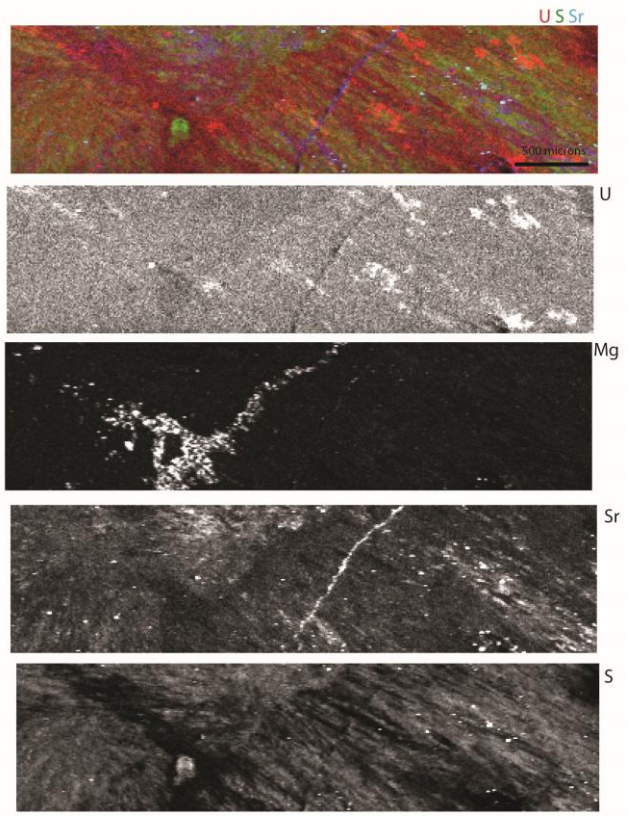
U S Sr
500 microns
U
Mg
Sr
S

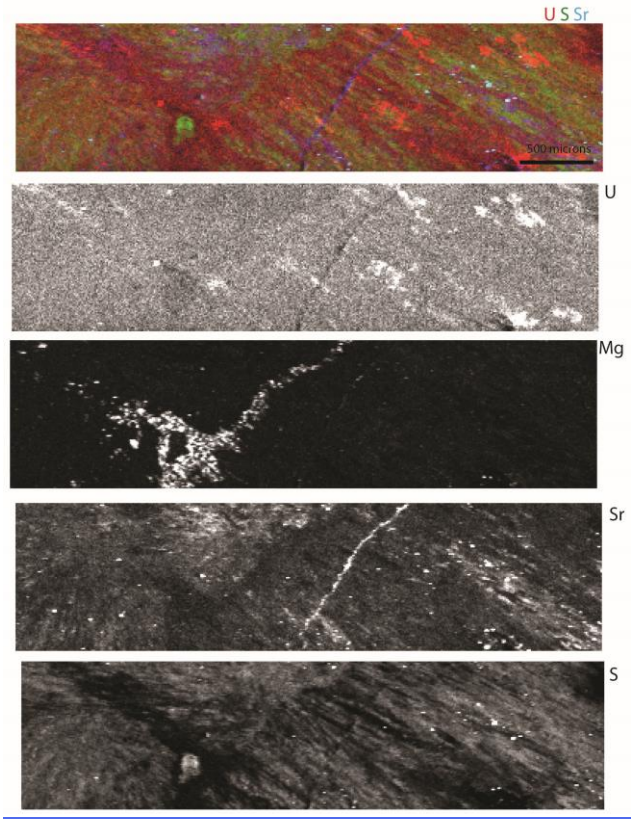

Figure ~~8~~7. Tender Energy Range (TES) synchrotron XRF maps of the Walnut Canyon slab shown in Fig. 3-6. The panels are labeled with the elements they represent. The top map is a RGB map where red is U, green is S and blue is Sr (note scale bar on the bottom right of the RGB image is 100 microns). The brightest areas in the U map are artifacts from diffraction. The best preserved areas are an olive green.

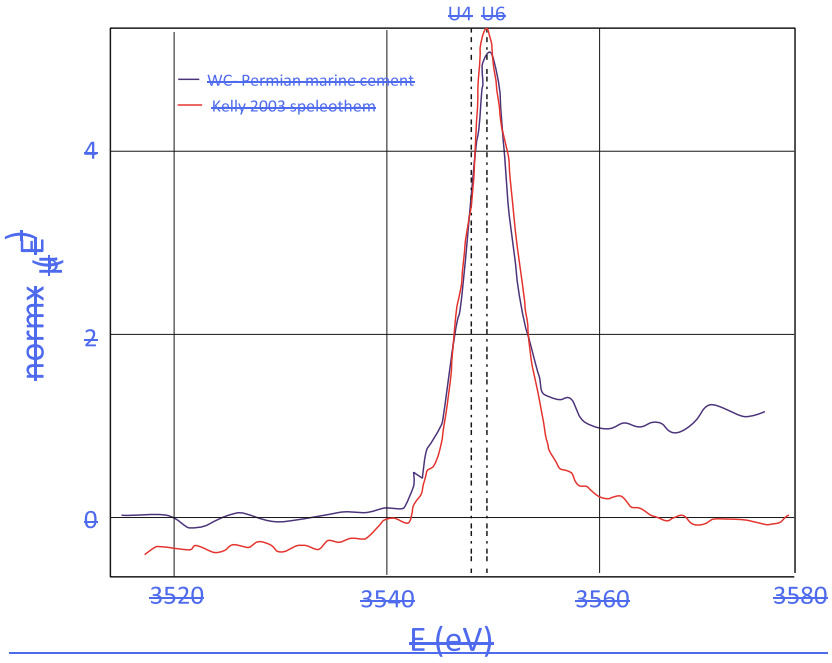
U4 U6
WC_Permian marine cement
Kelly 2003 speleothem
4
2
0
3520
3540
3560
3580
E (eV)

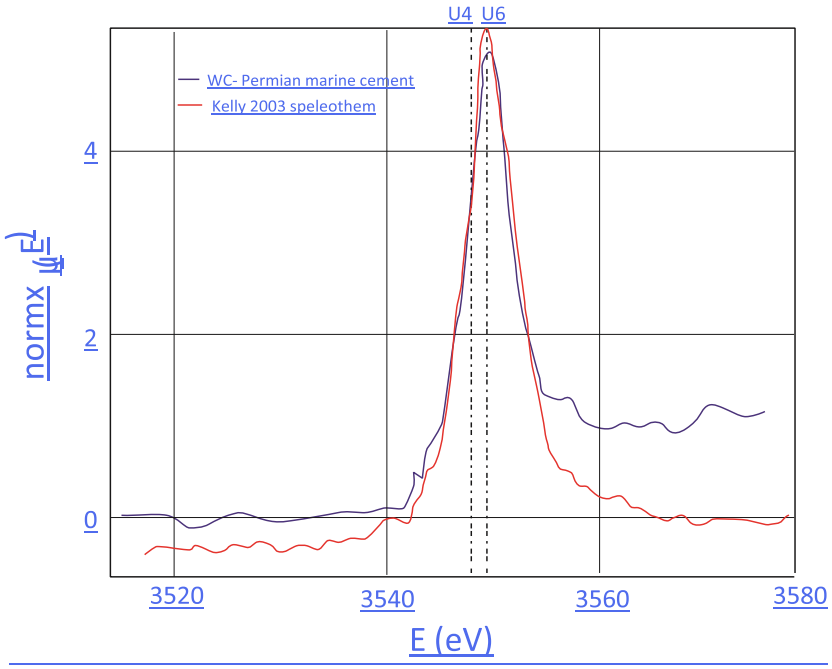

Figure 98. M5 edge X-ray absorption spectroscopy, 20 scans (15 sec each) showing that uranium is in the oxidized state. The TES beamline has a monochrometer that is very stable, allowing hours worth of scanning without drift. Speleothem from a cave in Austria Kelly et al. (2003) that has U(VI) for reference.

Figure ~~10~~9. Hand specimen of a Barstow Formation tufa sample that is large enough to slab and share as a secondary LAcarb ~~standard~~reference material.

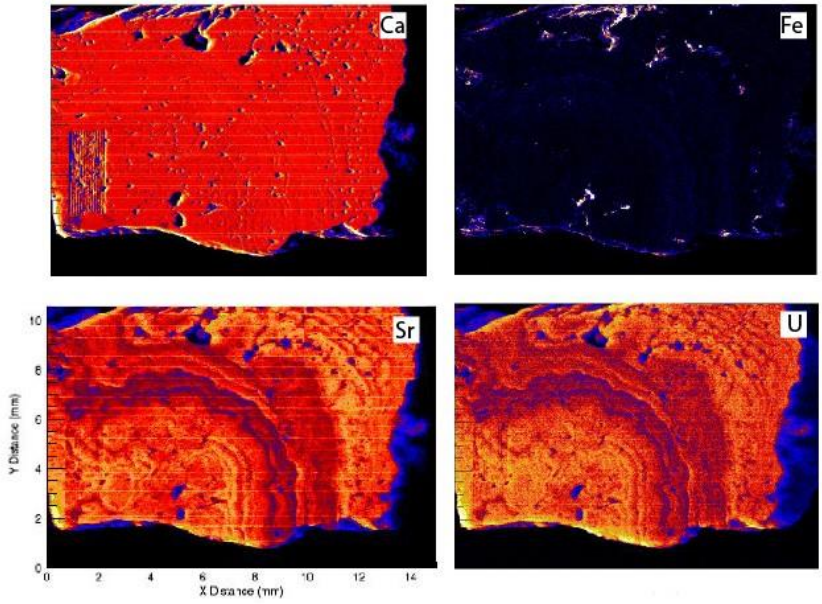
Ca
Fe
Sr
U
Y Distance (mm)
X Distance (mm)
0
2
4
6
8
10
12
14

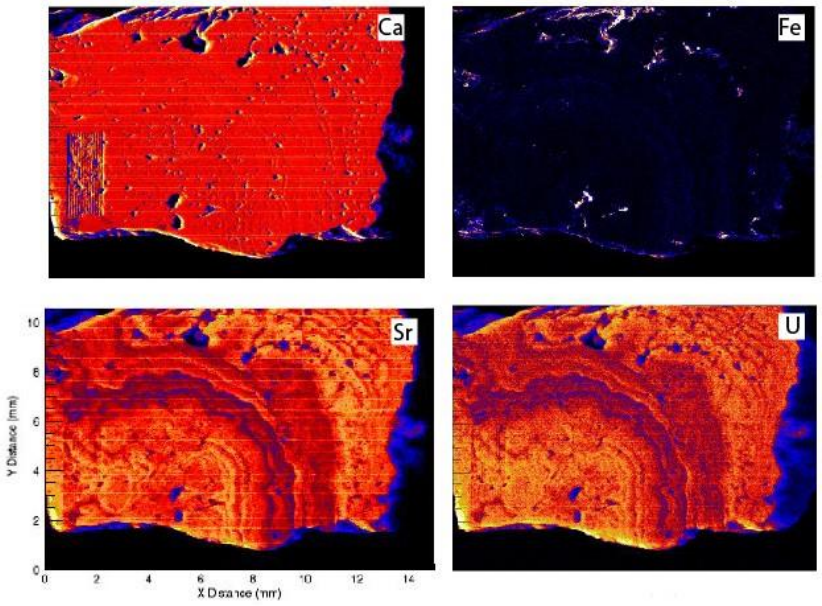

Figure ~~11~~10. On the fly synchrotron XRF maps of Ca, Fe, Sr and U for a slab of Barstow tufa. This in not the sample that is being characterized for a LAcarb ~~standard~~reference material, but it serves to show the relationships between U and Sr.

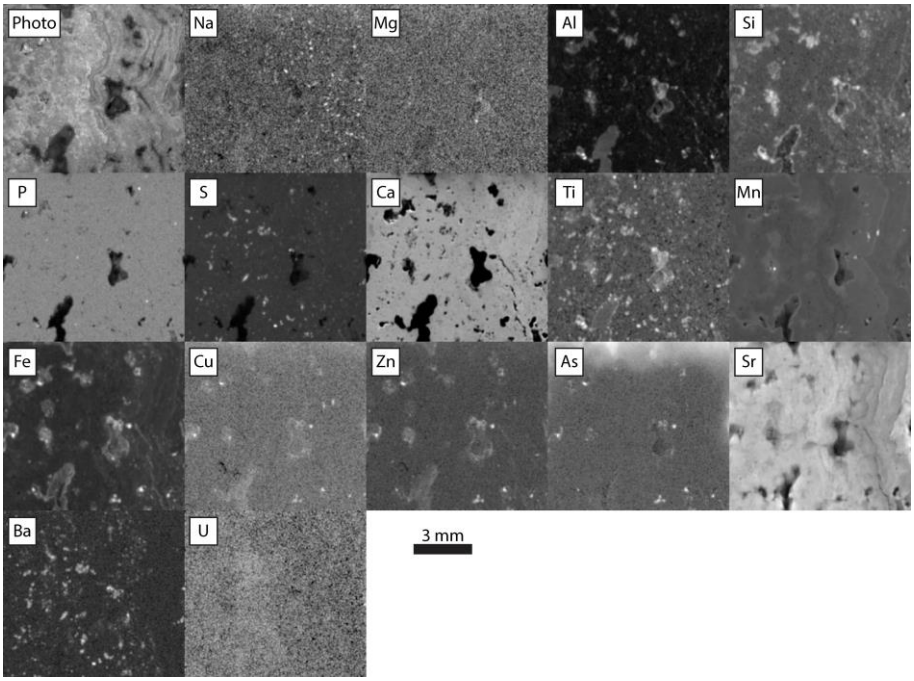
Photo
Na
Mg
Al
Si
P
S
Ca
Ti
Mn
Fe
Cu
Zn
As
Sr
Ba
U
3 mm

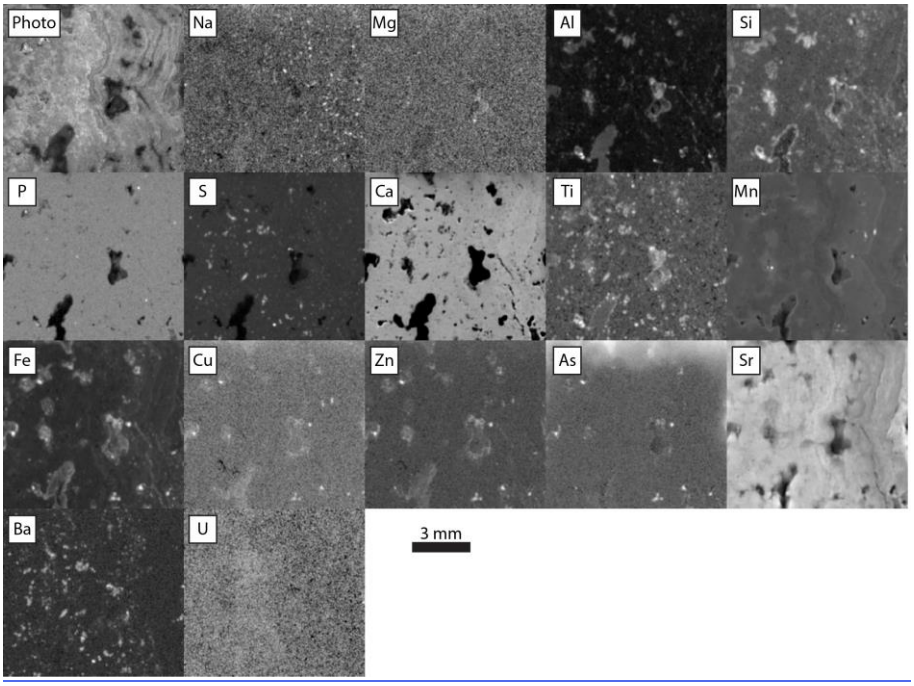
Photo
Na
Mg
Al
Si
P
S
Ca
Ti
Mn
Fe
Cu
Zn
As
Sr
Ba
U
3 mm

Figure ~~12~~11. Relative intensities of emission regions for each element detected in Barstow tufa, imaged at 25 µm pixels with 400 ms/pixel dwell time and 1.5 s.d. gaussian blur. Each panel is gamma and contrast adjusted to emphasize gradients between textures. Na through Fe data collected with no incident radiation filter. Cu through U data collected with incident radiation filtered with 100 µm Al, 50 µm Ti, 20 µm Cu foil.

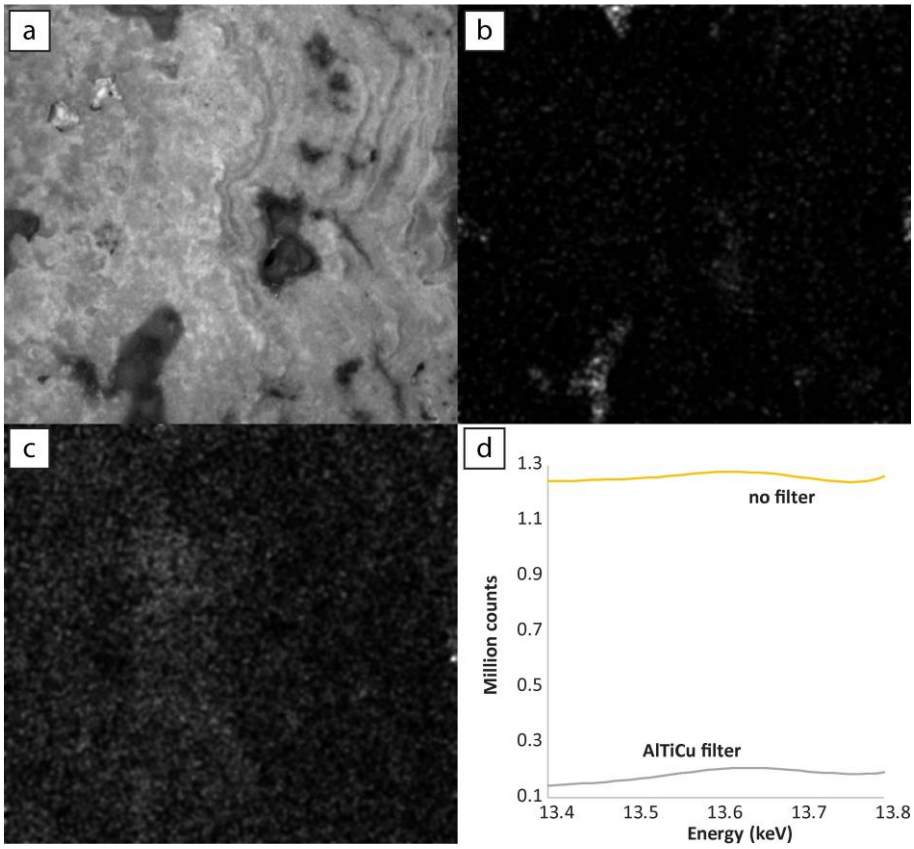

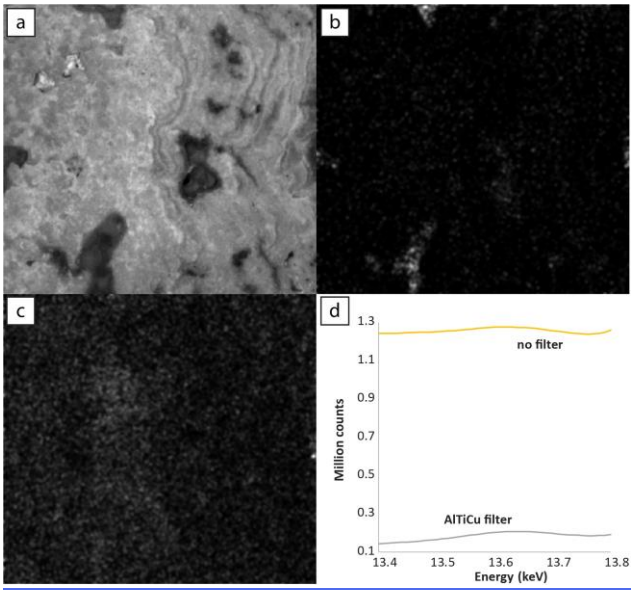

Figure ~~13~~12. Comparison of U-L α maps of Barstow tufa, imaged at 25 µm pixels with 400 ms/pixel dwell time and 1.5 s.d. gaussian blur. (a) Sample image. (b) No incident radiation filter. (c) Incident radiation filtered with 100 µm Al, 50 µm Ti, 20 µm Cu foil. (d) Sum spectra of total counts in U-L α line region.

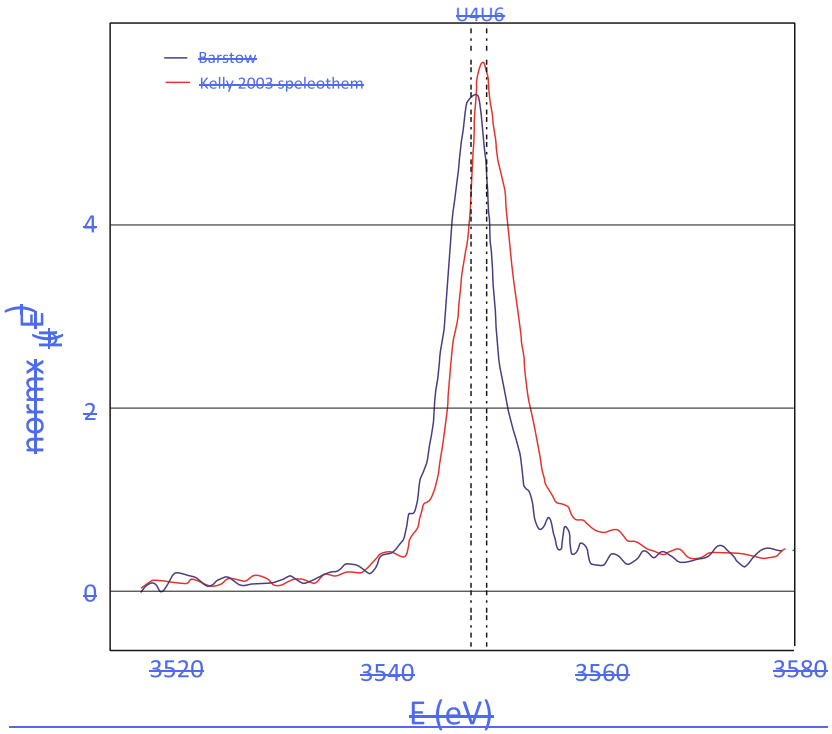

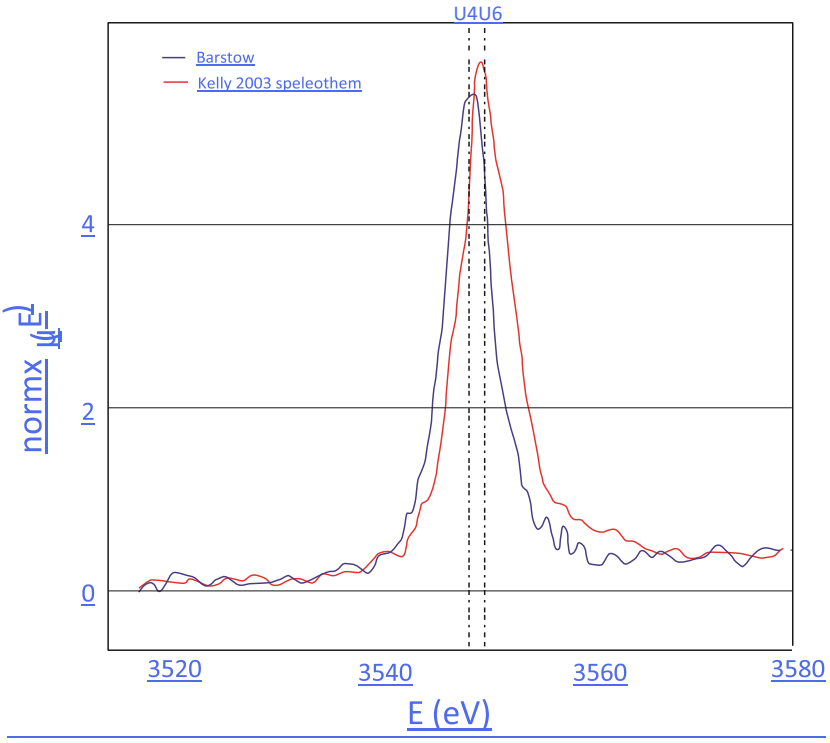

Figure ~~14~~13. Uranium M5 edge spectroscopy showing that uranium is in the reduced state; for reference, the U(VI) speleothem of (Kelly et al., 2003). Both measured at the TES beamline as described in Figure 9.

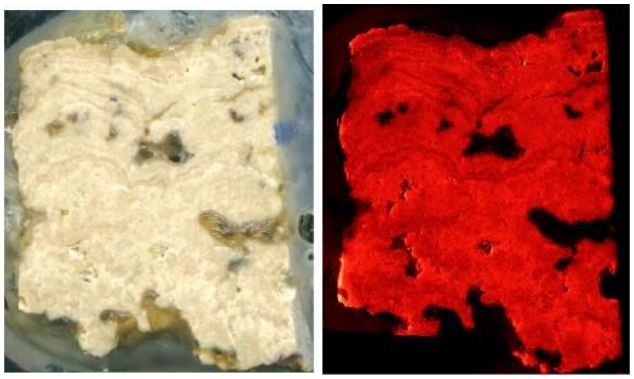

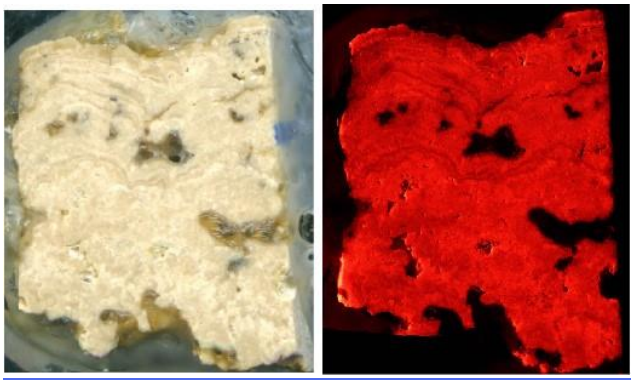

Figure ~~15~~14. Slab from the Bartow Formation tufa sample that is being characterized for a possible secondary LAcarb standard. The fine laminae are like those described by Becker et al. (2001). The left image is a scan of the slab. The right image is a CL photomosaic from 360 images. Generally, the more micritic areas are brighter luminescence and the sparry layers have a duller luminescence.

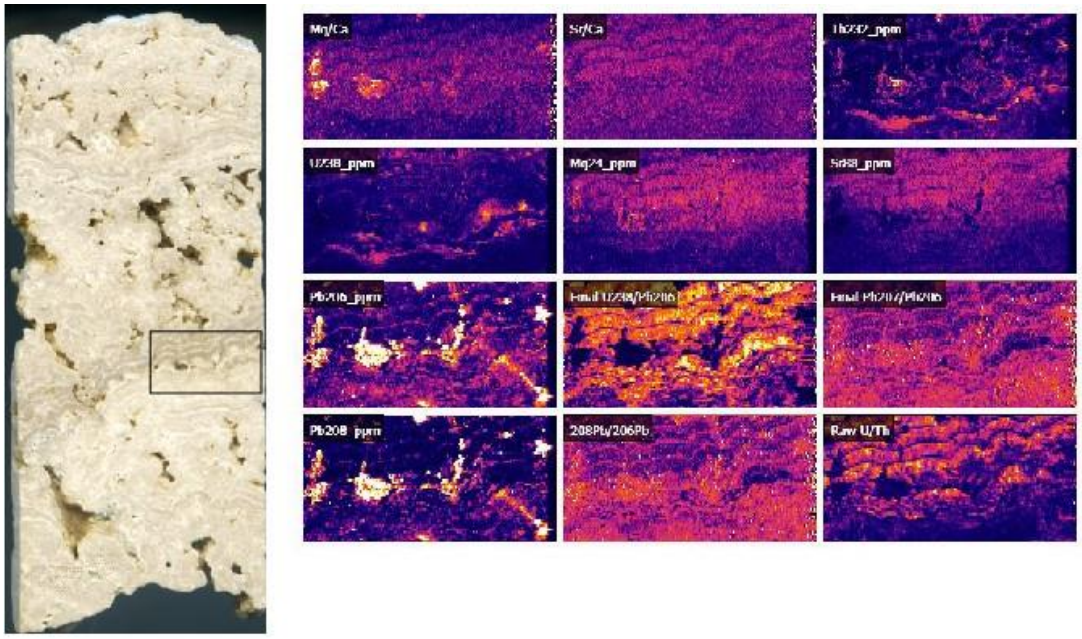

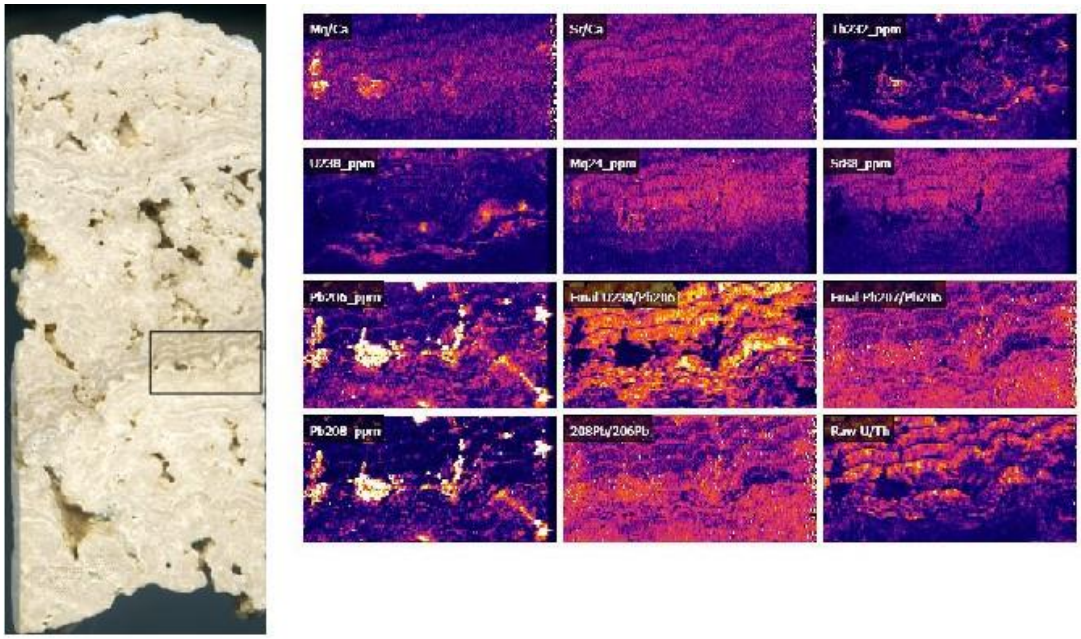

Figure 15. ~~Figure 16.~~ Slab of the Barstow tufa, approximately 1 cm wide. The box shows the location of the LA maps.

Sr >12,500 ppm

Sr> 12,500 ppm, 208Pb< 1ppm

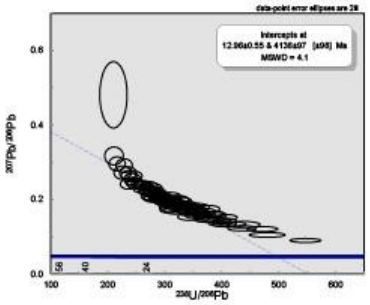

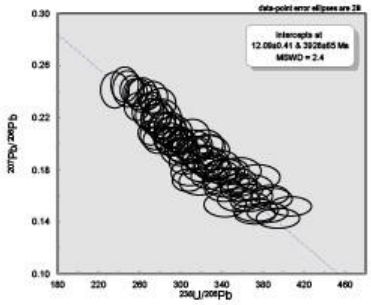

Sr> 12,500 ppm, age 14-17 Ma

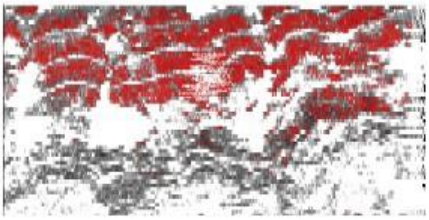

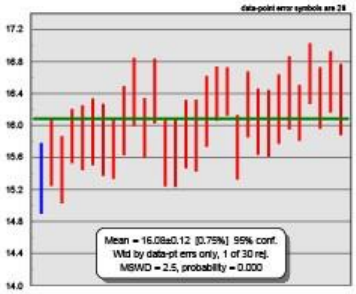

~~Figure 17.~~

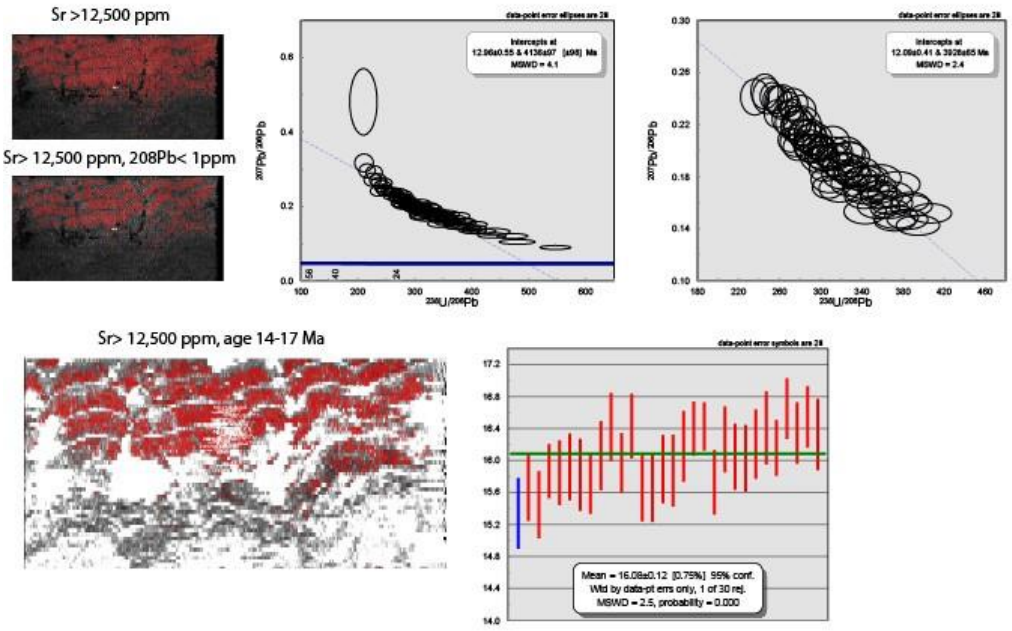

Figure 16. Sr concentration map used to select pixels for the sparry calcite in the Barstow tufa. In the top left map, the red marks the pixels that are over 12,500 ppm Sr. The map below, has the same ~~critera~~criteria plus the ^{208}Pb is less than 1 ppm. The first isochron plot is a binning of all of the pixels that meet this second ~~critera~~criteria without removing tails. The second isochron has the top and bottom 10% tails removed. The bottom map is the $^{206}Pb/^{238}U$ age map and the red pixels are greater than 12,500 ppm Sr and between 13-17 Ma. The probability plot is based on binning those pixels.


METRIC 1 2 3 4 5 6 7 8


1 cm

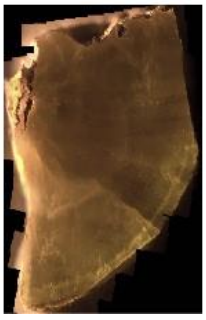

Figure ~~18~~17. Hand samples of the Turkana dolomite sample, both came from an area where carbonates were coating tree trunks. The big sample is from a very large cavity that was filled by calcite, then the yellow dolomite that is peeking out and finally by a coating of grey calcite. The smaller triangular shaped sample has a bark texture on the outside and appears to have precipitated in the cavity between three logs. The thickness of the dolomite layer is about 2 cm and it coats every surface in this paleo log pile. The small slabs come from the smaller of the two samples. The image on the left is the scanned slab used for XRF studies, and the one on the right is a CL photo ~~mossaic~~mosaic with 459 photos.

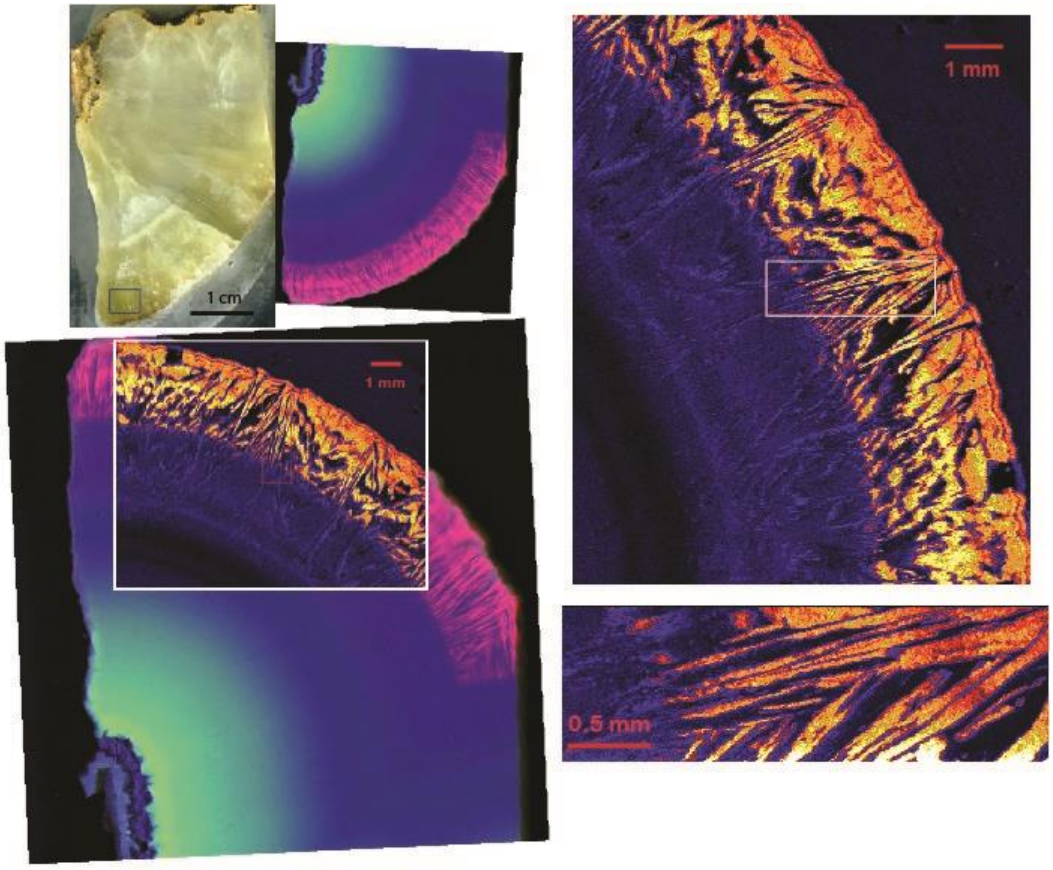
1 cm
1 mm
1 mm
0.5 mm

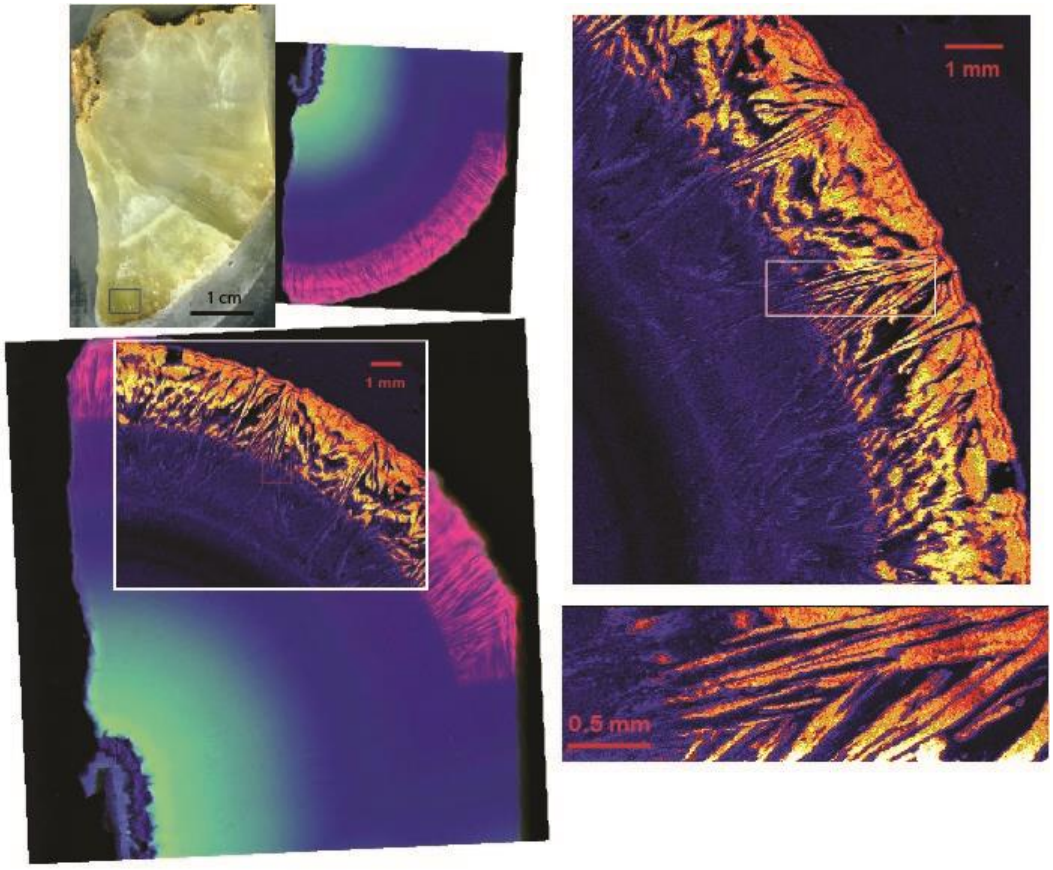

Figure ~~19~~18. Slab of the dolomite with on the fly synchrotron XRF images. The rectangle at the bottom of the sample is the approximate location of the LA maps in Figure 21. Directly to the right of the slab image is a RGB (USrCa) map from beamline XFM at the NSLS II. The images on the right are maps of U from TES. On the lower left, the TES U map is overlain on the same area that was mapped at XFM. The XFM mapping was done at 17 keV with a 10 micron beam and a 10 micron step size, and a counting time of 0.1 seconds. The large TES map was made at 3550 eV with an 18 micron beam, 20 micron pixels, counted for 0.3 seconds. The detail map on the bottom right was also made at 3550 eV with a 4 micron beam, 3.75 micron pixels, counting for 0.3 seconds.

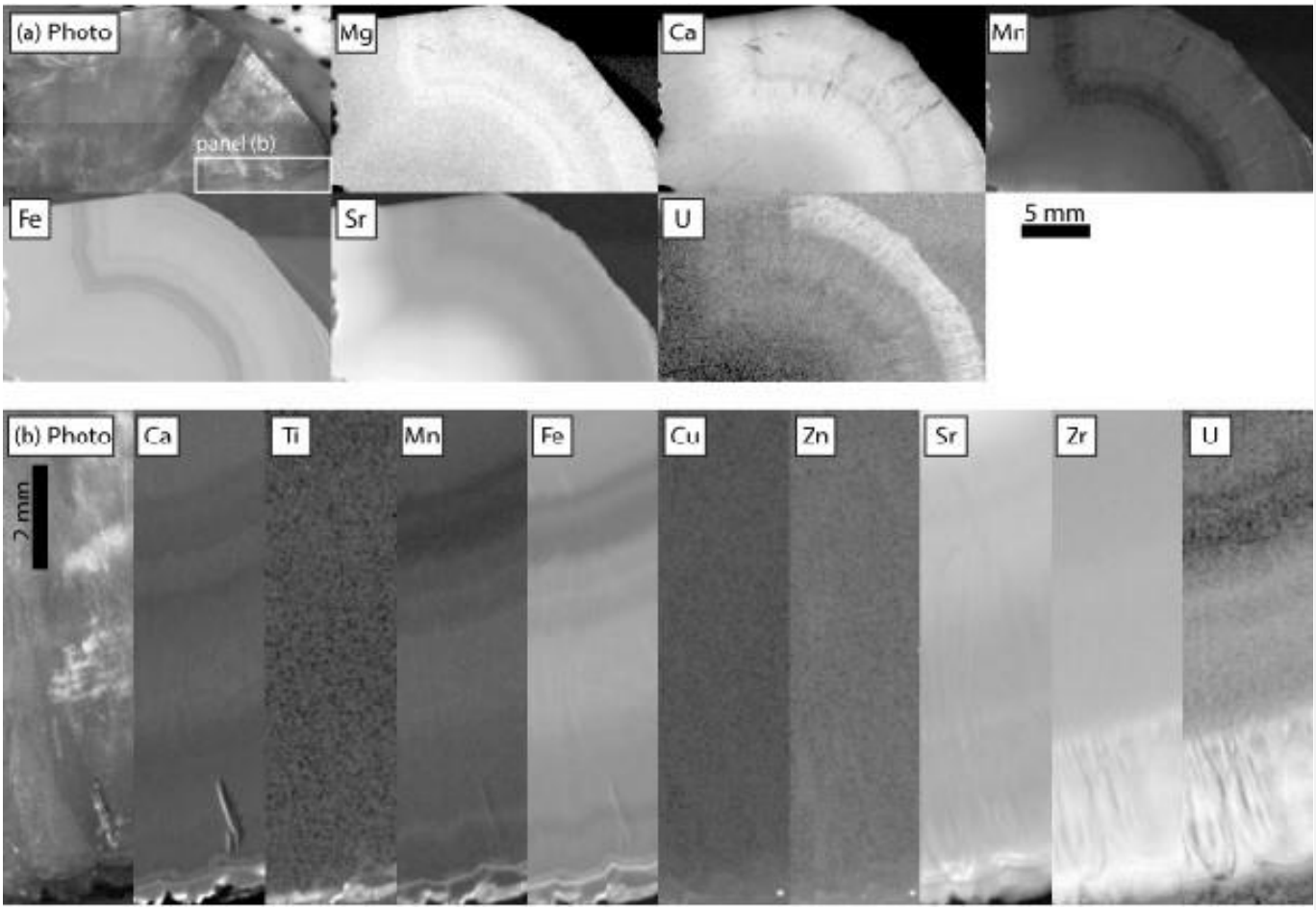
(a) Photo
Mg
Ca
Mn
panel (b)
Fe
Sr
U
5 mm
(b) Photo
Ca
Ti
Mn
Fe
Cu
Zn
Sr
Zr
U
2 mm

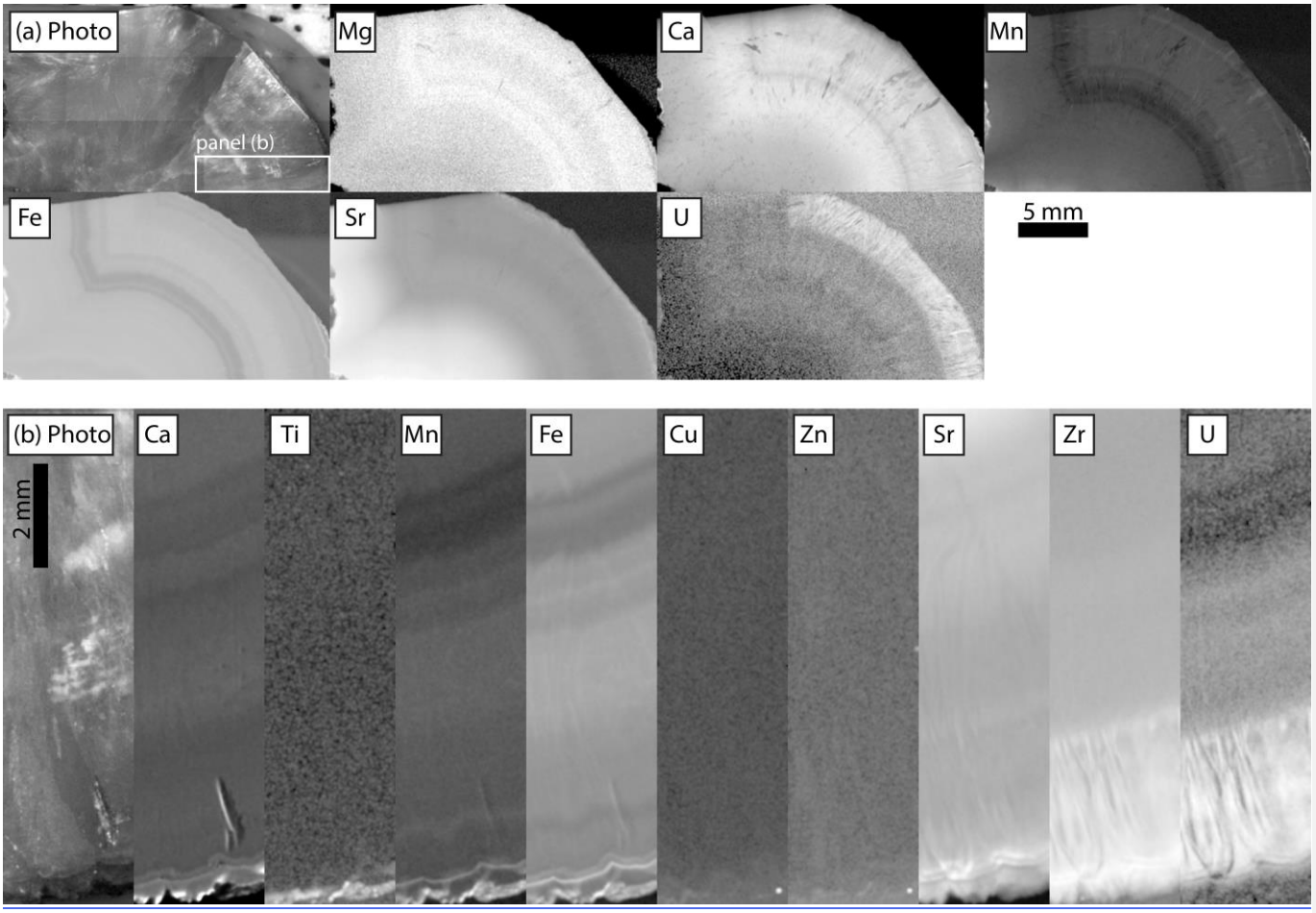

Figure ~~20~~19. Relative intensities of emission regions for each element detected in Turkana Dolomite. Each panel is gamma and contrast adjusted to emphasize gradients between textures. (a) No incident radiation filter, imaged at 25 µm pixels with 120 ms/pixel dwell time and 1.5 s.d. gaussian blur, with box indicating region re-mapped with filter shown in panel b. (b) Incident radiation filtered using 100 µm Al, 50 µm Ti, 20 µm Cu foil, imaged at 20 µm pixels with 900 ms/pixel dwell time and 1.5 s.d. gaussian blur.

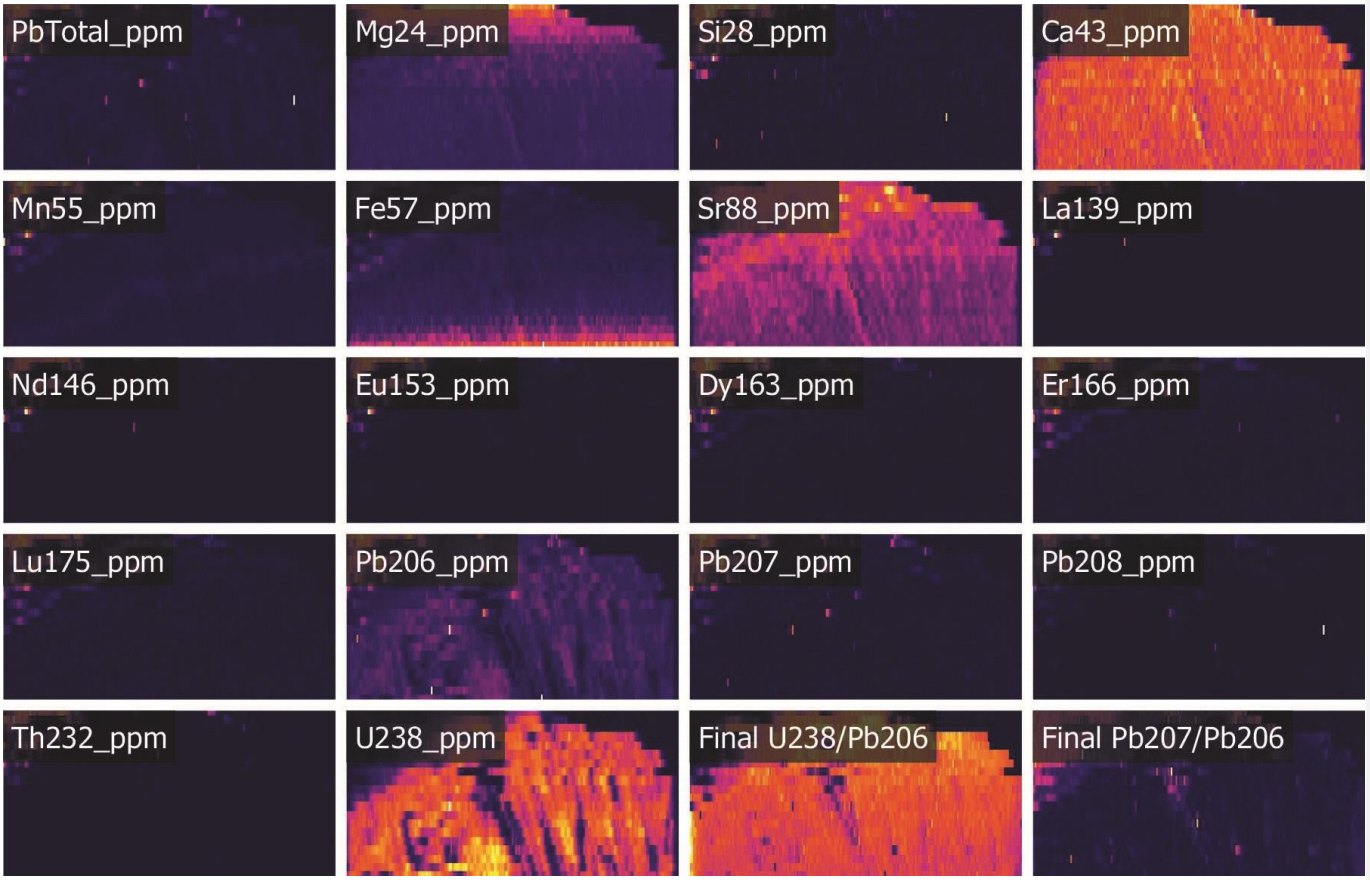
PbTotal_ppm
Mg24_ppm
Si28_ppm
Ca43_ppm
Mn55_ppm
Fe57_ppm
Sr88_ppm
La139_ppm
Nd146_ppm
Eu153_ppm
Dy163_ppm
Er166_ppm
Lu175_ppm
Pb206_ppm
Pb207_ppm
Pb208_ppm
Th232_ppm
U238_ppm
Final U238/Pb206
Final Pb207/Pb206

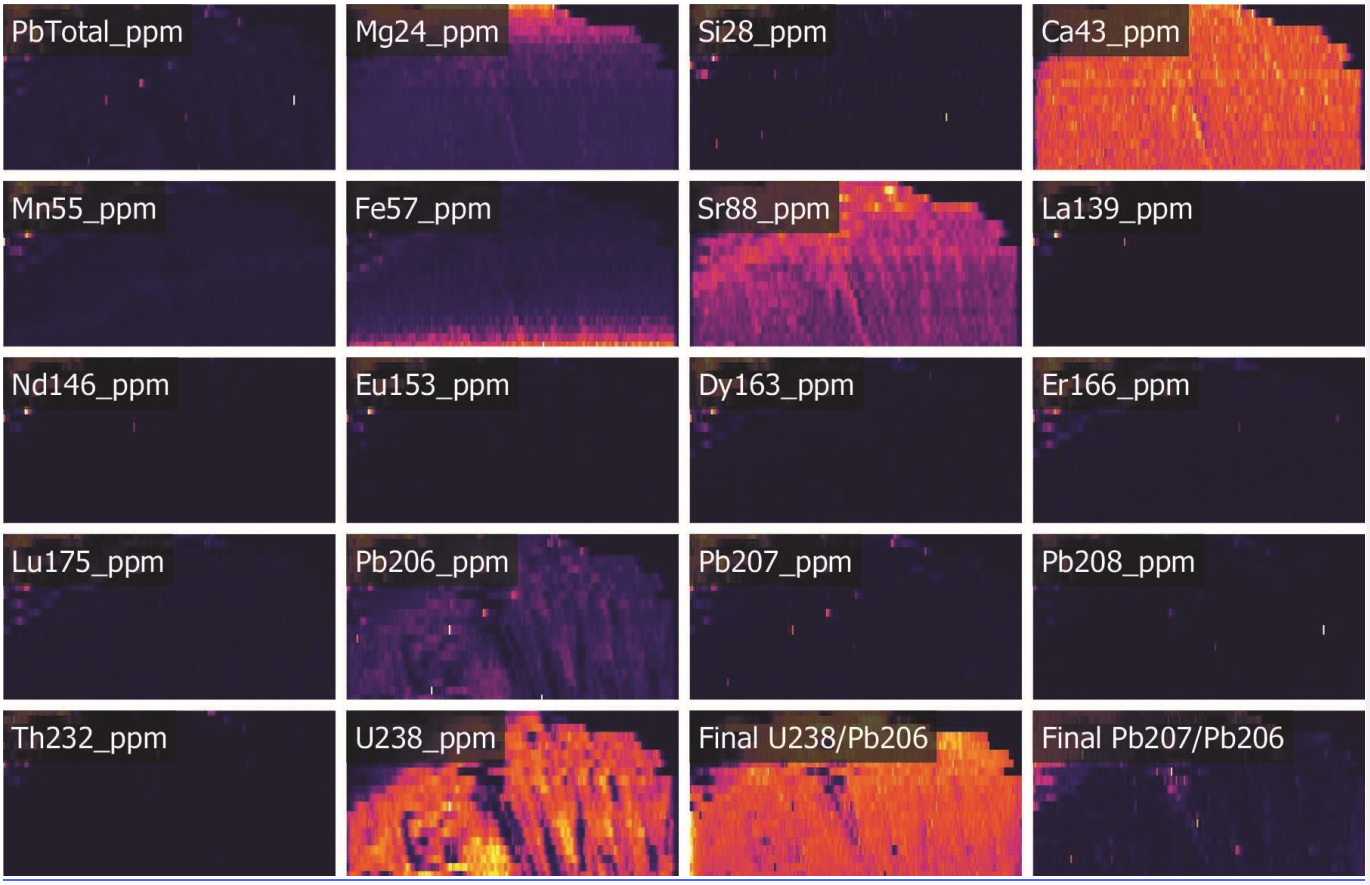

Figure ~~21~~20. Laser Ablation ICPMS maps of the TBW dolomite. U is high concentration, while Pb and Th are low. The REE are also low abundance. The U/Pb ratio is very favorable.

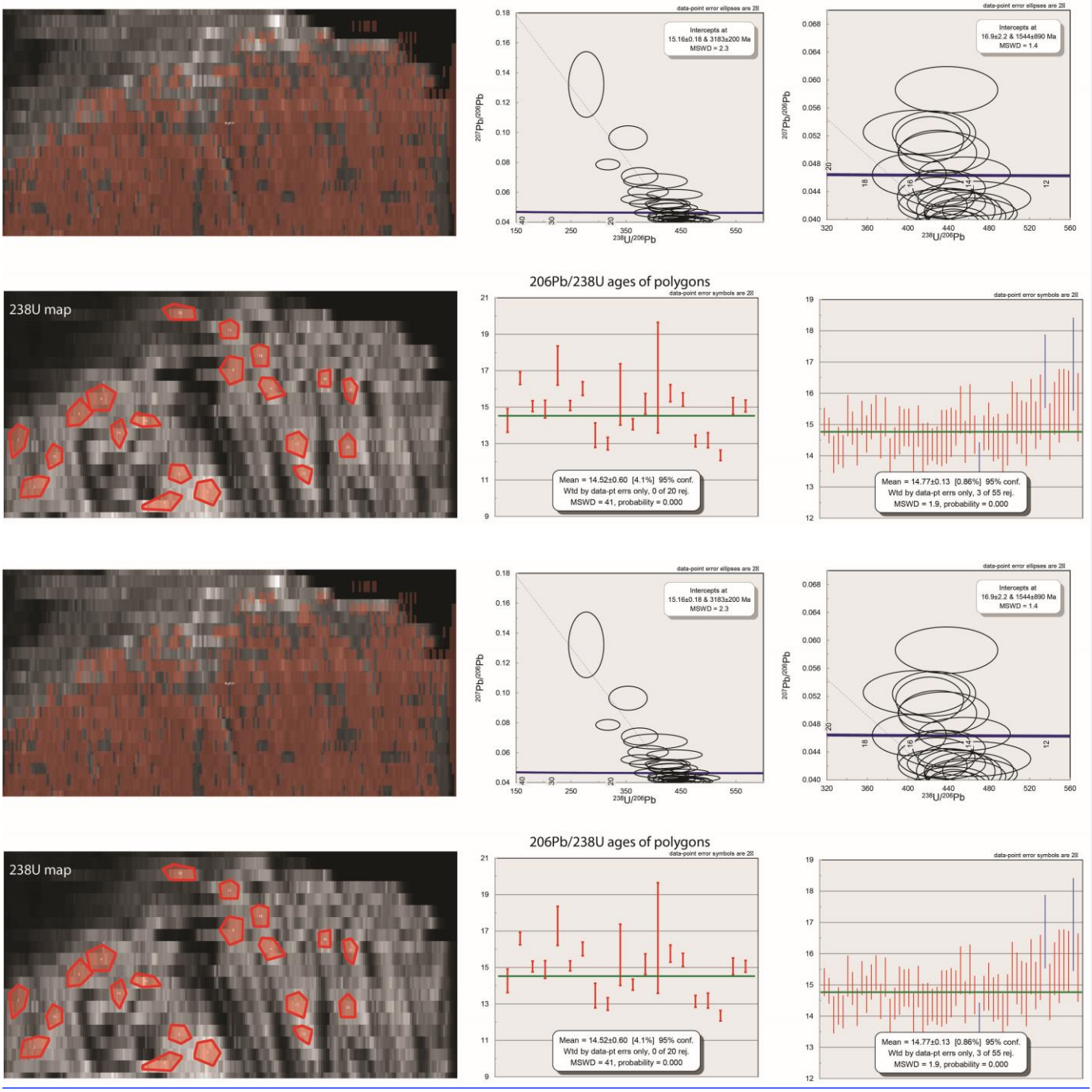

Figure ~~22~~21. Map of U. Regions selected based on U concentration. $^{206}Pb/^{238}U$ ages of each region shown on a probability plot.

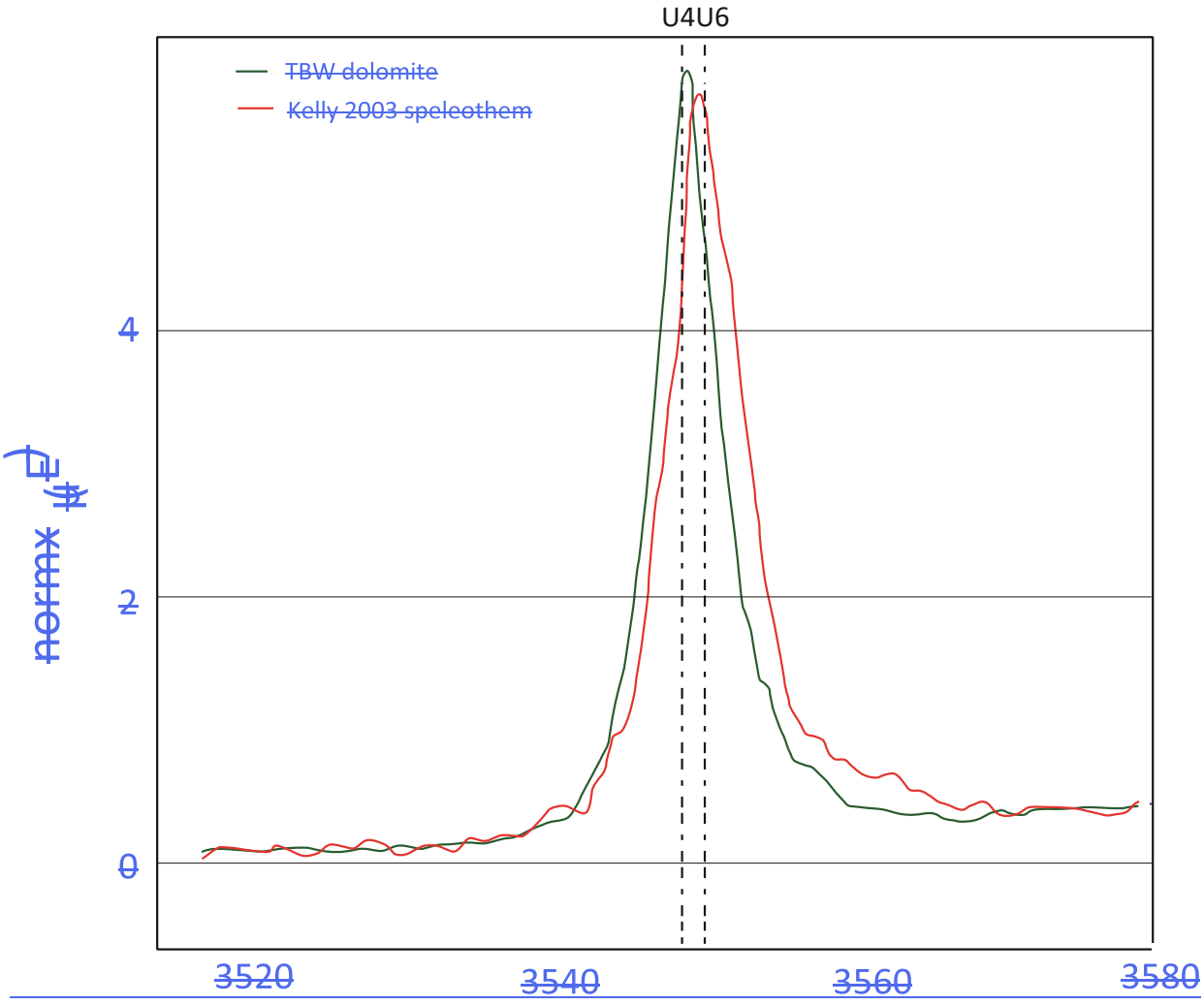
U4U6
TBW dolomite
Kelly 2003 speleothem
4
2
0
3520
3540
3560
3580

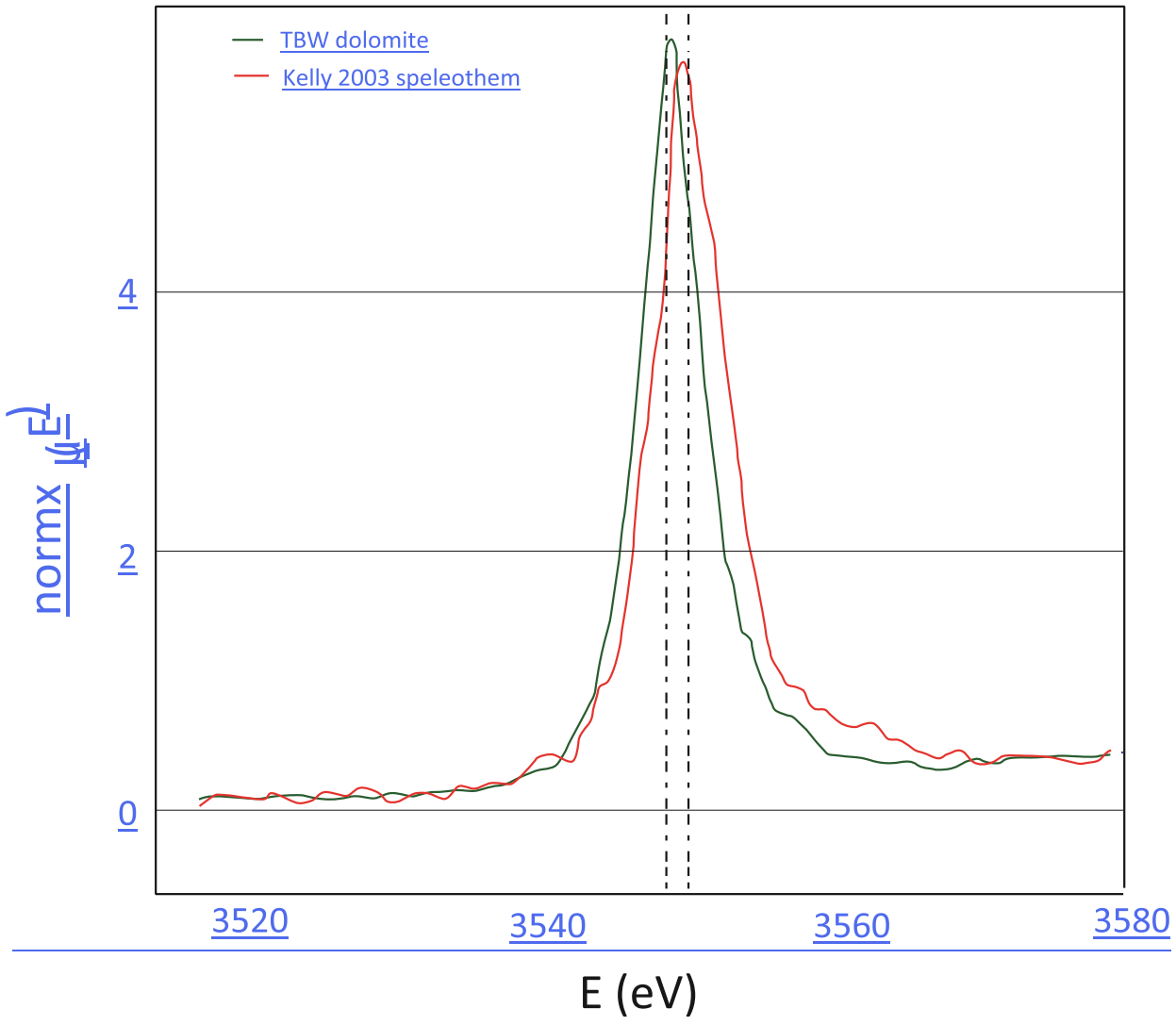

Table 1. $^{87}Sr/^{86}Sr$ from aliquots of the Barstow tufa run by Thermal Ionization Mass Spectrometry

sample	$^{87}Sr/^{86}Sr$	2SD
BT1	0.720423	0.000011
BT2	0.721038	0.000011
BT3	0.719877	0.000011

Table 2. $^{87}Sr/^{86}Sr$ from aliquots of the Turkana dolomite run by Thermal Ionization Mass Spectrometry

sample	$^{87}Sr/^{86}Sr$	2SD

TBWi-1	0.703309	0.000011
TBWi-2	0.703299	0.000011
TBWo-1	0.703306	0.000011
TBWo-2	0.703312	0.000011